1963

Comparison of Theoretical, Laboratory and Field Discharge Ratings for a Closed Conduit Spillway

Fred A. Schmer

COMPARISON OF THEORETICAL, LABORATORY AND FIELD DISCHARGE RATINGS FOR A CLOSED CONDUIT SPILLWAY

BY

FRED A. SCHMER

A thesis submitted
in partial fulfillment of the requirements for the
degree Master of Science, Department of
Agricultural Engineering, South Dakota
State College of Agriculture
and Mechanic Arts

March, 1963

COMPARISON OF THEORETICAL, LABORATORY

AND FIELD DISCHARGE RATINGS FOR

A CLOSED CONDUIT SPILLWAY

This thesis is approved as a creditable, independent investigation by a candidate for the degree, Master of Science, and is acceptable as meeting the thesis requirements for this degree, but without implying that the conclusions reached by the candidate are necessarily the conclusions of the major department.

William J. Lytle

Thesis Adviser

Dennis L. Snow

Head of the Major Department

ACKNOWLEDGMENTS

It is scarcely possible in this short space to give an adequate statement of appreciation to all who have had a direct or indirect share in this presentation. The author is particularly indebted to Professor Dennis Moe and Associate Professor William F. Lytle of the Agricultural Engineering Department, South Dakota State College, for their encouragement and technical assistance which made possible the completion of this investigation. Appreciation is also extended to all other members of the Agricultural Engineering staff for their assistance when needed and to Agricultural Engineering graduate student, Richard Pedersen, for his assistance in obtaining all laboratory data.

The author wishes to thank governmental organizations, Soil Conservation Service and the U. S. Geological Survey, for their generous assistance in supplying needed field instrumentation and their cooperation in supplying technical assistance and suggestions.

The author acknowledges sincere appreciation to his wife, Lynda, for the time spent reviewing, rough typing, and final typing of this presentation.

FAS

TABLE OF CONTENTS

	Page
INTRODUCTION	1
REVIEW OF LITERATURE	8
OBJECTIVES AND SCOPE	12
MODEL DESIGN	13
Dimensional Analysis	13
Model-prototype Scale Ratio	16
LABORATORY APPARATUS	19
Spillway Construction	19
Approach Channel	30
Spillway Conduit Cradle	31
Discharge Collection	32
Discharge Recorder	32
Stage Recorder	35
Differential Manometer	37
LABORATORY TEST PROCEDURE	42
Personnel Requirements	42
Data Collection	42
LABORATORY ANALYSIS	46
Stage and Discharge Recordings	46
Manometers	46
FIELD APPARATUS AND TESTING PROCEDURE	52
Description and Location of the Watershed	52

Discharge Structure 52
Detention Basin Elevation Recordings 54
Discharge Recordings 57
RESULTS 64
Rating Curve 64
Spillway Conduit 75
Spillway Vortices 78
V-notch 79
Future Investigation 79
CONCLUSIONS 81
LITERATURE CITED 83
APPENDICES 85
Appendix A. Definition of Symbols 86
Appendix B. Manometer Data Analysis 89
Appendix C. Instrumentation Circuit Diagrams 94
Appendix D. Model Loss Coefficients 98

LIST OF FIGURES

Figure		Page
I.	Detention Basin No. 11, Scott Creek Watershed, March, 1960	5
II.	Typical Closed Conduit Spillway Installation	7
III.	Complete Laboratory Apparatus	20
IV.	Model Spillway Section	21
V.	Installed Spillway Section Above the Tank	22
VI.	Installed Spillway Below the Tank	23
VII.	Detailed Drawing of Model Spillway Section	24
VIII.	Simulated Corrugated Metal End Section	29
IX.	Typical Laboratory Discharge and Head Pool Elevation Recording	33
X.	Laboratory Photoelectric Cell Timing Unit	34
XI.	Instrumentation for Laboratory Discharge Recording	36
XII.	Stage Recorders for Approach Channel	38
XIII.	Piezometer Tap Location	40
XIV.	Manometer Board	41
XV.	Detailed Drawing of the Field Riser Section	53
XVI.	Prefabricated House Containing Stage Recorder	55
XVII.	Typical Continuous Detention Basin Stage Recording	58
XVIII.	Typical Continuous Field Discharge Recording on Parshall Flume	59
XIX.	Downstream End of Parshall Flume Under Capacity Flow Conditions	61
XX.	Parshall Flume Installed on Watershed	61

XXI. Predicted Rating Curve From Model Data 65

XXII. Theoretical, Laboratory, and Field Rating Curve Comparisons 69

XXII-a. Logarithmic Plot of Full-Pipe Flow Rating Curves . 77

XXIII. Schematic of Manometer Apparatus 90

XXIV. Schematic Circuit Diagram for the Discharge Recorder 95

XXV. Circuit Diagram for the Photoelectric Cell Unit . 96

XXVI. Basic Synchro System Circuit Diagram 97

LIST OF TABLES

Table		Page
1.	Final Corrugated Metal Simulation Texts	27
2.	Random Sample of Laboratory Data	47
3.	Relative Elevations of Specific Model Locations	49
4.	Typical Loss Coefficients and Reynolds Numbers	51
5.	Broad-crested Weir Coefficients	72
6.	Model Loss Coefficients	99

INTRODUCTION

One can easily write the story of man's growth in terms of his epic concerns with water. The control of natural stream flow was the logical beginning of mankind's efforts to provide his fields and himself with water. It is sometimes said that the control of water for the purpose of irrigation probably preceded even civilization itself. There is still some divergence of opinion as to whether the first successful efforts to control water were made in Egypt or in Mesopotamia since remains of prehistoric irrigation works have been found in both countries, and the dating of events in this period is very inexact. Each country appears to have contained ample natural resources, and neolithic evidence of relatively thick population indicates that natural water control and irrigation development were necessary to support the population. The transition from the prehistoric age of stone to that of copper can be considered to have occurred some four-thousand years before the Christian era, and, therefore, one can conclude that extensive irrigation systems existed in both countries long before this time (19).

A further stride forward in control of water flow is found in the use of artificial conduits for the conveyance of water over reaches in which the natural topography would not permit the use of open cuts. There are traces of remarkably adequate systems built by the Pheonicians in Syria and Cyprus involving tunnels through rock and pressure conduits across valleys. Jerusalem was supplied water

in early times by a closed conduit system constructed some thousand years before Christ. From the pool of Solomon two conduits led to the city, the lower of which is twenty miles long and crosses the valley of Hinnom on arches and is still complete.

Inasmuch as only incomplete pictorial and physical records of these early achievements remain, one can only guess as to the actual principles of flow possessed by these early designers. It is logical that these structures were constructed instinctively with little actual knowledge of flow principles. One can generally conclude that their hydraulics of early antiquity was purely an art with no scientific basis beyond the principle of successive approximation toward a desired end. A further example of early hydraulics theory is noted in the words of Frontiners, an early (40-103 A.D.) Roman military engineer (19).

> Whence it appears that the amount measured by me is none too large: the explanation of this is, that the more impetuous stream of water increases the supply, since it comes from a large and rapidly flowing river.

This is a rather inconclusive statement. Nevertheless, it implies investigation of the dependence of discharge on velocity. Although this understanding of the continuity law is far from being quantitative or even qualitative, it indicates that development of the various basic concepts of hydraulics was being attempted. These early attempts to formulize the basic concepts of hydrodynamics resulted in further extensive investigation by many philosophers of hydrodynamic principles, and the present basic laws of hydraulics were

subsequently theorized and deduced.

Leonardo da Vinci (1452-1519) expressed qualitatively the elementary principle of continuity, observed and sketched many basic flow phenomena, and suggested designs for hydraulic machinery. Daniel Bernoulli (1700-1782) experimented and wrote on many phases of fluid motion, coining the name "hydrodynamics." Bernoulli also devised the manometry technique and adopted primitive energy principles to explain velocity-head indication. The basic energy principle bears the name of Bernoulli today.

With the basic concepts of hydrodynamics deduced, new and more reliable mathematical and experimental theorization has been subsequently developed. Although hydrodynamics has progressed immensely in the last one-hundred years, only the frontier of hydrodynamics has been discovered, and a vast region is still left for further theorization and development.

Although the development of hydrodynamics has been extensive in the nineteenth century, the effect of the control of runoff to retain and store water and to prevent erosion had not been fully realized until the early 1930's. Presently in this country, the control of runoff on watersheds is extensively being employed to conserve and to retain runoff. (A watershed is defined as the specific drainage area of a system of natural streams or rivers.)

In the past decade, it has also become evident that the scientific control and management of runoff on small watersheds is

necessary if a desirable, overall, soil and water conservation program is to be attained. (A small watershed contains less than 250,000 acres for the specific drainage area.) The development and control of these small watershed areas has yielded invaluable endowments for many rural communities. Water from protected watersheds with desirable conservation practices is a natural resource that is growing in importance and value everywhere where water shortage is evident as an asset in industrial development, recreational facilities, stable rural population, and higher agricultural income (2).

Figure I is a photograph showing the ability of the conservation practices and the detention basin in retarding the excess runoff of March, 1960, on the Scott Creek Watershed located in Union County, South Dakota. The photograph is an aerial view of the large detention basin number eleven located on the lower part of Scott Creek Watershed. The investigation of theoretical and experimental evaluation of the discharge characteristics of the mechanical spillway located on this particular detention basin is the primary interest of this presentation. The component parts of a detention basin are the storage area, earth dam, grassed emergency flood spillway, and mechanical spillway.

The mechanical spillway is the means by which excessive runoff beyond the storage capacity of the detention basin is conveyed through the detention dam. The ideal mechanical spillway

Figure I. Detention Basin No. 11 Scott Creek Watershed, March, 1960

for a small watershed detention basin should possess these three characteristics: 1. simple and inexpensive to manufacture, 2. easy to install, and 3. good hydraulic characteristics (9). The major hydraulic problem encountered in the design of these spillways is to obtain maximum discharge with a minimum head because of the limited head usually available on these structures. In the past, many designs of mechanical spillways have been investigated by various people and organizations, and it is generally agreed that some type of closed conduit spillway appears to be the best adopted for the small watershed detention basin.

The closed conduit spillway consists of a vertical section called the riser and nearly horizontal conduit called the barrel, and a connection of the barrel to the riser called the transition section. The assembled parts form an "L" with the internal angle slightly larger than 90 degrees. Figure II is a schematic diagram of the installation of a typical closed conduit spillway for a small watershed detention basin.

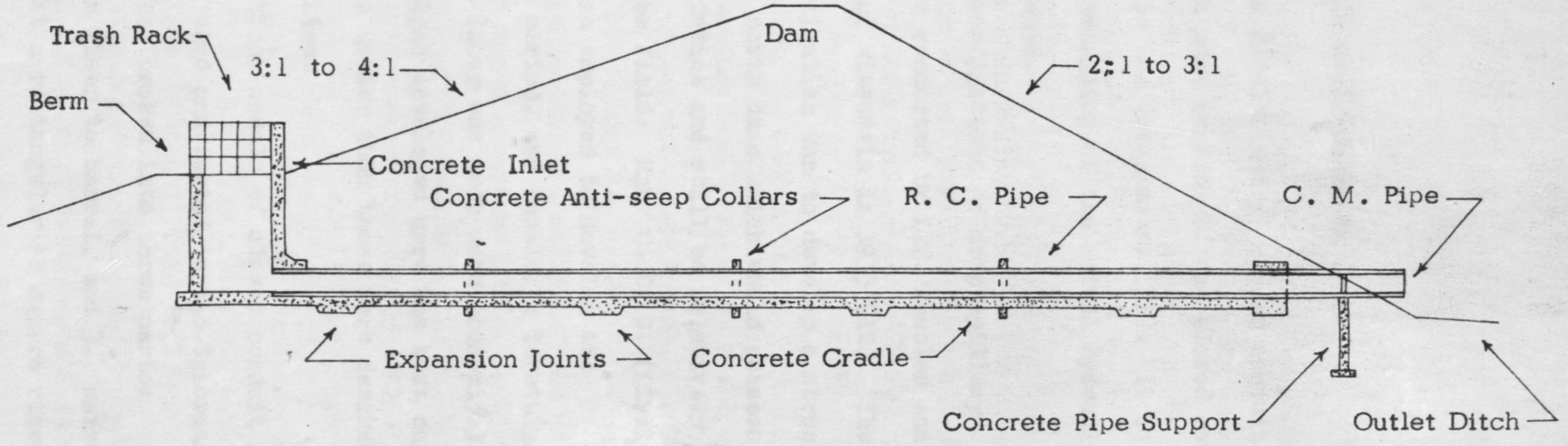

Figure II. Typical Closed Conduit Spillway Installation

REVIEW OF LITERATURE

From the history of the development of closed conduit hydraulics, it is evident that some version of the closed conduit spillway existed as far back as the Pheonicians (19). It is also evident that very little understanding of the actual hydraulic phenomena of the spillway existed.

One of the earliest investigations of drop spillway structures in this country was conducted by L.H. Kessler and his associates of the University of Wisconsin in 1933 (12). The primary purpose of this investigation was to develop a structure to convey water through small earth dams which would possess desirable hydraulic characteristics and still be relatively inexpensive and easy to install in the field. Many C. C. C. (Civilian Conservation Corps) people were employed to develop the conservation programs at this period, and Kessler's investigation was governed by the fact that labor was much more economical than material. Therefore, the designs developed were the best suited under these imposed conditions rather than those more desirable from the standpoint of hydraulics.

In Kessler's investigation, models of closed conduit spillways were constructed of wood and tested in the laboratory. The laboratory investigation was broken into three parts: 1. inlet, 2. transition from riser to barrel, and 3. barrel. It was generally concluded that a rectangular or square riser with

some type of beveled lip was most desirable. The transition from riser to barrel was constructed of a curved section without square corners. The barrel was limited to precast concrete pipe because of availability and cost. The prototype characteristics were determined by model-prototype dimensional analysis, and very little, if any, actual model-prototype comparisons were made.

In 1934, the U. S. Department of Agriculture established the S. C. S. (Soil Conservation Service) and later in 1953 the A. R. S. (Agricultural Research Service). The establishment of these two organizations greatly increased the soil and water conservation practices in the country and thereby increased the need for investigations of small spillway structures. In the early 1950's, the Federal Government developed the Pilot Watershed Program under which pilot watersheds were developed throughout the country. The Watershed Protection and Flood Prevention Act of 1954 (Public Law 566 as amended) is the program under which attempted present scientific control of small watersheds is administered. Under this authorization, local people must initiate conservatory districts containing the area to be benefited by the intended development and administer the watershed treatment. The Federal Government provides technical aid and pays all of the construction costs applicable to flood prevention. Local people must administer the program, arrange for easements and rights-of-way to permit installation of improvements and contract for construction work, and provide adequate maintenance

for all installations. Because of the active part the Federal Government has taken in the development of these small watershed programs, investigations to obtain a desirable spillway for these watersheds were initiated.

In 1950, Blaisdell at the University of New Hampshire conducted studies on square risers and circular barrels. He studied the theory, effect of size of structure, effect of slope, and the effect of circulation around the headwall for closed conduit spillways, with respect to the head-discharge relationship (4). In the 1950's, Blaisdell and his associates at the University of Minnesota's St. Anthony Falls Hydraulic Laboratory continued investigations on the closed conduit spillway, and the present design procedures of the S. C. S. are based on Blaisdell's investigations. It is the opinion of the author that the design criteria for these relatively small spillways is based mostly on installation and construction factors rather than on desirable hydraulic characteristics. Therefore, the hydraulic characteristics of these structures were determined after the design criteria was developed. Blaisdell's investigations have included very little actual model-prototype comparisons.

Nelson (15), in 1956 in connection with the Illinois State Water Survey Division, investigated the hydraulics of closed conduit spillways. He was mainly interested in determining the various types of flows encountered between no flow and full-pipe flow. From

this investigation, Nelson concluded that five flow regimes, with respect to head on the spillway, exist: 1. weir flow with clinging nappe, 2. weir flow with aerated nappe, 3. orific flow, 4. vortex or slug flow, and 5. full-pipe flow.

In the past few years, J. A. Replogle and associates at the University of Illinois have been conducting model and prototype tests of an existing drop spillway structure. A paper (16) presented at the 1961 A. S. A. E. (Agriculture Society of Agricultural Engineers) winter meeting summarized the results of this investigation. Replogle's investigation indicates an amazingly close relationship between the field, laboratory, and theoretical evaluation of the closed conduit spillway rating curve. The investigation has compiled many years of field discharge records, and the conclusions obtained are substantiated in all realms of the investigation. Other investigations have also been conducted on closed conduit structures, but model-prototype comparisons have not been economically feasible.

OBJECTIVES AND SCOPE

Comparing theoretical and laboratory model discharge rating curves for a small discharge structure is relatively easy, but obtaining reliable field data on the prototype for additional comparison sometimes presents formidable problems. Generally the construction and testing of a model and a corresponding prototype to obtain comparisons is not econimically feasible. In this particular case, the reverse order of development was employed, and a model was constructed of an existing field structure. Data was obtained from both the laboratory and field studies and theoretical, laboratory, and field comparisons made. It was the desire of the author to substantiate criteria on which future design of mechanical spillways for small watershed detention basins could be based.

Objectives of this investigation:

1. To investigate the ability of the V-notch, cast in the front lip of the spillway in removing small flows.

2. To investigate the effect, on the discharge rating curve, of a corrugated metal end section on the precast concrete conduit.

3. To investigate the three types of flow, (weir flow, slug flow, and full-pipe flow), generally assumed to exist in this type of structure.

4. To make theoretical, laboratory, and field comparisons of the existing closed conduit spillway on the watershed.

5. To obtain a discharge rating curve for the field closed conduit spillway.

MODEL DESIGN

A model is a device which is so related to a physical system that observations on the model may be used to predict accurately the performance of the physical system. The physical system for which the predictions are to be made is called the prototype (14). The model and prototype must behave similarly and qualitatively, so that a quantitative relationship may be established between them, and observations of the performance of the model can then accurately predict the performance of the prototype. By the employment of the theory of similitude which is developed by dimensional analysis, a quantitative relationship between model and prototype can be developed, and accurate prototype predictions can theoretically be accomplished. Unfortunately, complete similarity is generally not economically feasible, and omissions of "minor" parameters must be allowed to develop a quantitative relationship between model and prototype.

Dimensional Analysis

In 1915, Buckingham brought before the engineering world the principal tool of dimensional analysis, by which one accomplishes the organization of variables, called the Buckingham (7) II theorem. In general, the only variables that can influence fluid motion are of the following categories (18): 1. geometrical boundary conditions, 2. kinematic and dynamic characteristics of flow, and

3. fluid properties. By selection and grouping of the variables involved in these categories, eight dimensionless Π terms can be obtained which fall into three basically different types of dimensionless parameters: 1. those defining the boundary conditions, 2. those characterizing the basic flow pattern, and 3. those pertaining to the action of weight, viscosity, surface tension, and elasticity. The latter group of variables are known respectively as the Froude, Reynolds, Weber, and Cauchy numbers (18).

In this particular investigation, there are basically three types of flow occurring: 1. very low flow of which surface tension would be the primary consideration, 2. weir flow of which weight would be the primary consideration, and 3. full-pipe flow of which viscosity would be the primary consideration. Since the investigation was interested in relatively high flows, the model prototype similitude theory was basically concerned with the effects of weight and viscosity.

The pertinent variables affecting the weight (partial pipe flow) phenomenon are:

D = diameter of pipe
e = roughness of pipe wall
V = average flow velocity
ρ = density of fluid
g = gravitation effect
d = average depth of flow

By application of the Π theorem to those variables, it can be shown that the Froude number ($V/\sqrt{gd}$) is the pertinent dimensionless term.

The pertinent variables affecting the viscosity (full-pipe flow) phenomenon are:

D = diameter of pipe
e = roughness of pipe well
V = average flow velocity
ρ = density of the fluid
μ = dynamic viscosity of the fluid

Likewise, by application of the Π theorem to these variables, it can be shown that the Reynolds number (ρ VD/μ) is the pertinent dimensionless term.

Therefore, if a complete model-prototype similarity is to be obtained, it is essential that both Reynolds and Froude numbers be the same in model and prototype. Assuming "g" to have the same magnitude in model and prototype, and assuming the Reynolds and Froude numbers the same, results in:

$$\frac{V_m}{V_p} = \frac{D_p \nu_m}{D_m \nu_p} = \frac{(g\, d_m)^{\frac{1}{2}}}{(g\, d_p)^{\frac{1}{2}}} \qquad (1)$$

Where:

$\nu = \mu/\rho$ = Kinematic viscosity

As can be seen by the foregoing discussion, it is physically impossible to have these pertinent dimensionless terms equated in model and prototype if the same fluid is to be used. Since fluids with the viscosity required to obtain this similarity are not economically feasible for this type of model study, it becomes necessary to deem one of these pertinent dimensionless terms as a "minor" term and regulate the model-prototype comparisons in

accordance with the "primary" dimensionless term. The velocities encountered in this model-prototype investigation will result in relatively large Reynolds numbers in the model and prototype. Since the slope of the Reynolds number versus friction factor curve (17) is relatively flat in the region encountered, it becomes logical to deem the Reynolds number as the "minor" parameter and evaluate the model-prototype relationship in accordance with the "primary" parameter, the Froude number.

Model-prototype Scale Ratio

Since it has previously been determined that the "primary" parameter of the model-prototype relation is the Froude number, some considerations of the Reynolds number must be employed to assure that the Reynolds number of the model is within the region that allows the Reynolds number variance to be neglected. In this investigation, one of the primary interests was to determine the effect of the relative roughness of the conduit in retarding full-pipe flow, and, therefore, the model-prototype scale ratio should be such that geometric similarity results between the respective roughnesses. The following procedure was employed in selecting the model-prototype ratio.

From the Froude relationship:

$$V_r = \frac{V_m}{V_p} = \sqrt{\frac{L_m}{L_p}} = \sqrt{L_r} \qquad (2)$$

By use of the Manning equation:

$$\frac{V_m}{V_p} = \frac{\left[(1.49/n)\ (R^{2/3})\ (S^{\frac{1}{2}})\right]_m}{\left[(1.49/n)\ (R^{2/3})\ (S^{\frac{1}{2}})\right]_p} \qquad (3)$$

Since the model and prototype are geometrically similar, the equation (3) reduces to:

$$\frac{V_m}{V_p} = \frac{n_p}{n_m}\left(\frac{R_m}{R_p}\right)^{2/3} \qquad (4)$$

This relationship has no bearing on the requirements of dynamic similarity, but it provides the basis for control of the roughness of a model in order to achieve dynamic similarity as indicated from the foregoing Froude relationship.

Combining equations (2) and (4), and replacing the length terms by hydraulic radius:

$$\frac{n_p}{n_m}\left(\frac{R_m}{R_p}\right)^{2/3} = \left(\frac{R_m}{R_p}\right)^{\frac{1}{2}} \qquad (5)$$

Or:

$$\frac{n_m}{n_p} = \left(\frac{R_m}{R_p}\right)^{1/6} = \left(L_r\right)^{1/6} \qquad (6)$$

Where:

n = Manning "n" value for roughness

$L_r = L_m/L_p$ = length ratio

Therefore, in order to select a model-prototype scale ratio, some assumptions must be made as to the roughness of the respective materials used to construct the model and prototype. A value of

Manning n = 0.009 for Lucite pipe was assumed (5). It can generally be assumed that the value of Manning "n" for precast concrete pipe ranges from 0.010 to 0.017 (7). With these assumed roughness values and the previously derived expression (equation 6), it can be calculated that the length ratio can vary from 1:2 up to 1:45 and still be within limits of accepted roughness values for precast concrete pipe. If a logical assumption of n = 0.014 for precast concrete pipe is made, the model-prototype length ratio would be 1:14.

With the specific prototype dimensions in mind and the available dimensions of Lucite pipe available, a model-prototype length ratio of 1:6 was selected. The author is aware of the fact that this length ratio probably will not result in the desired model roughness, but since the prototype roughness must be assumed and then checked by indirect methods, the model roughness can be easily adjusted to this assumed roughness without destroying any of the other criteria established by the Froude number.

LABORATORY APPARATUS

The laboratory apparatus used in this study was a combination of existing facilities in the hydraulics laboratory located in the Agricultural Engineering Building at South Dakota State College and the design and assembly of particular apparatus that was needed for this study. Figure III is a photograph of the complete laboratory apparatus used in this study.

Spillway Construction

Figure IV is a photograph of the finished spillway section before testing. The test model spillway was basically constructed of $\frac{1}{2}$-inch Lucite with other thicknesses utilized where definite additional thickness was desired. The appropriate spillway was precisionly cut and planned within $\pm$ 0.05 of an inch for all desired dimensions. The spillway was assembled with number 8 by 1-inch screws with silcon waterproofed grease in all joining sections. A number 29 drill bit was used to drill the Lucite, and threads were tapped for each screw. Figure V is a photograph of the installed spillway above the tank and Figure VI of the spillway below the tank. The bottom portion of the back of the spillway which contained the discharge conduit was made separate from the rest of the spillway to facilitate installation of the spillway in the approach channel tank. Figure VI shows this portion of the installed spillway. Figure VII is a detailed drawing of the spillway.

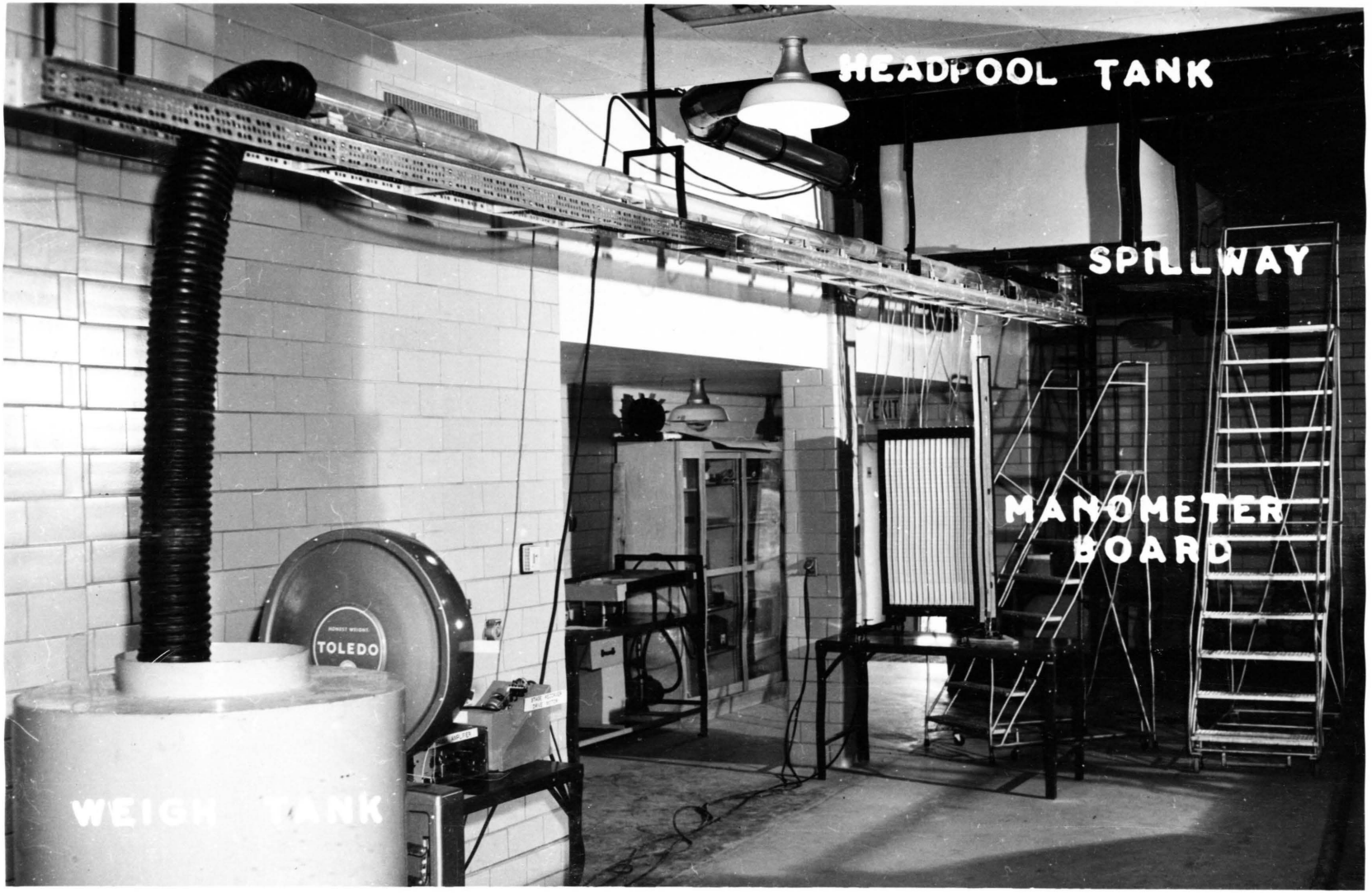

Figure III. Complete Laboratory Apparatus

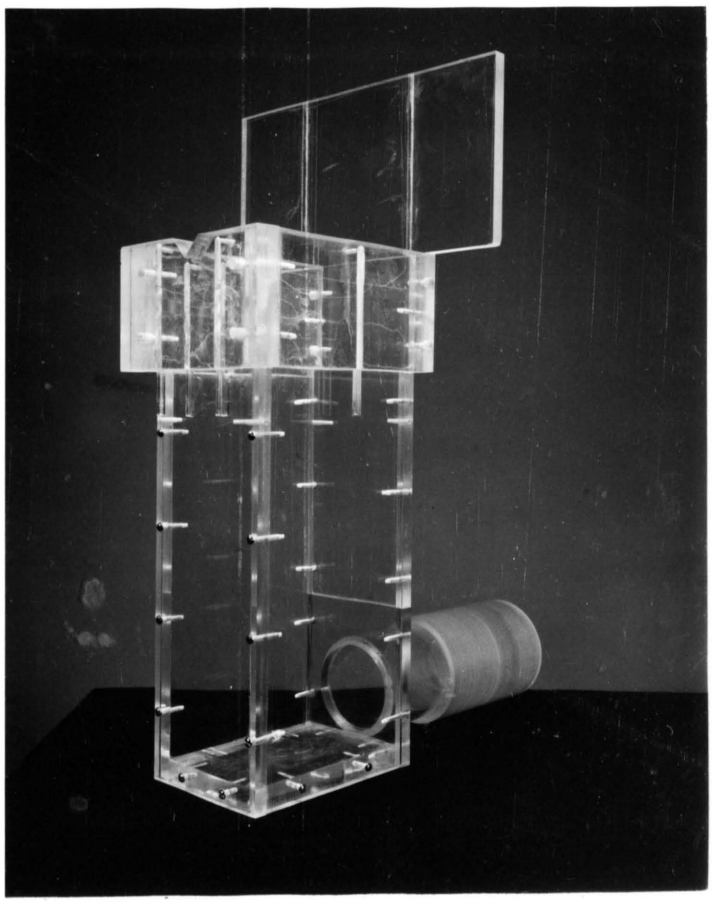

Figure IV. Model Spillway Section

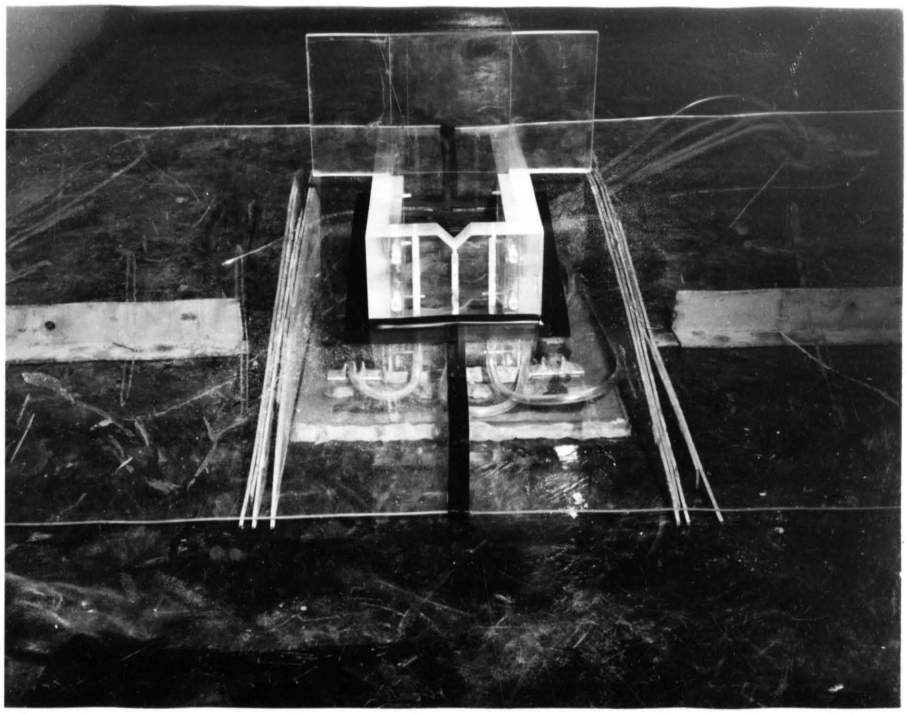

Figure V. Installed Spillway Section Above the Tank

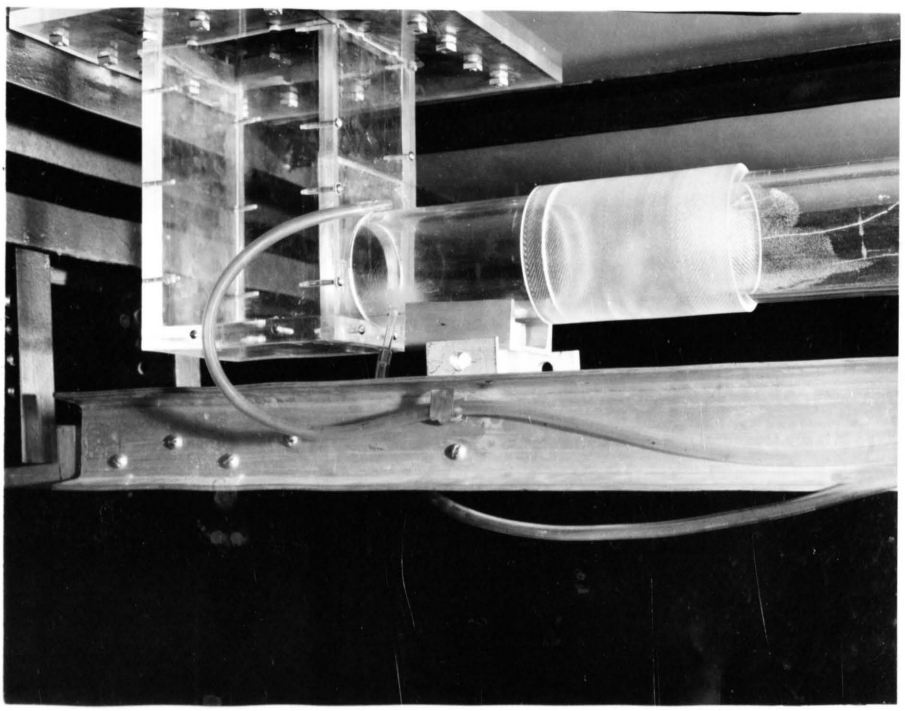

Figure VI. Installed Spillway Section Below the Tank

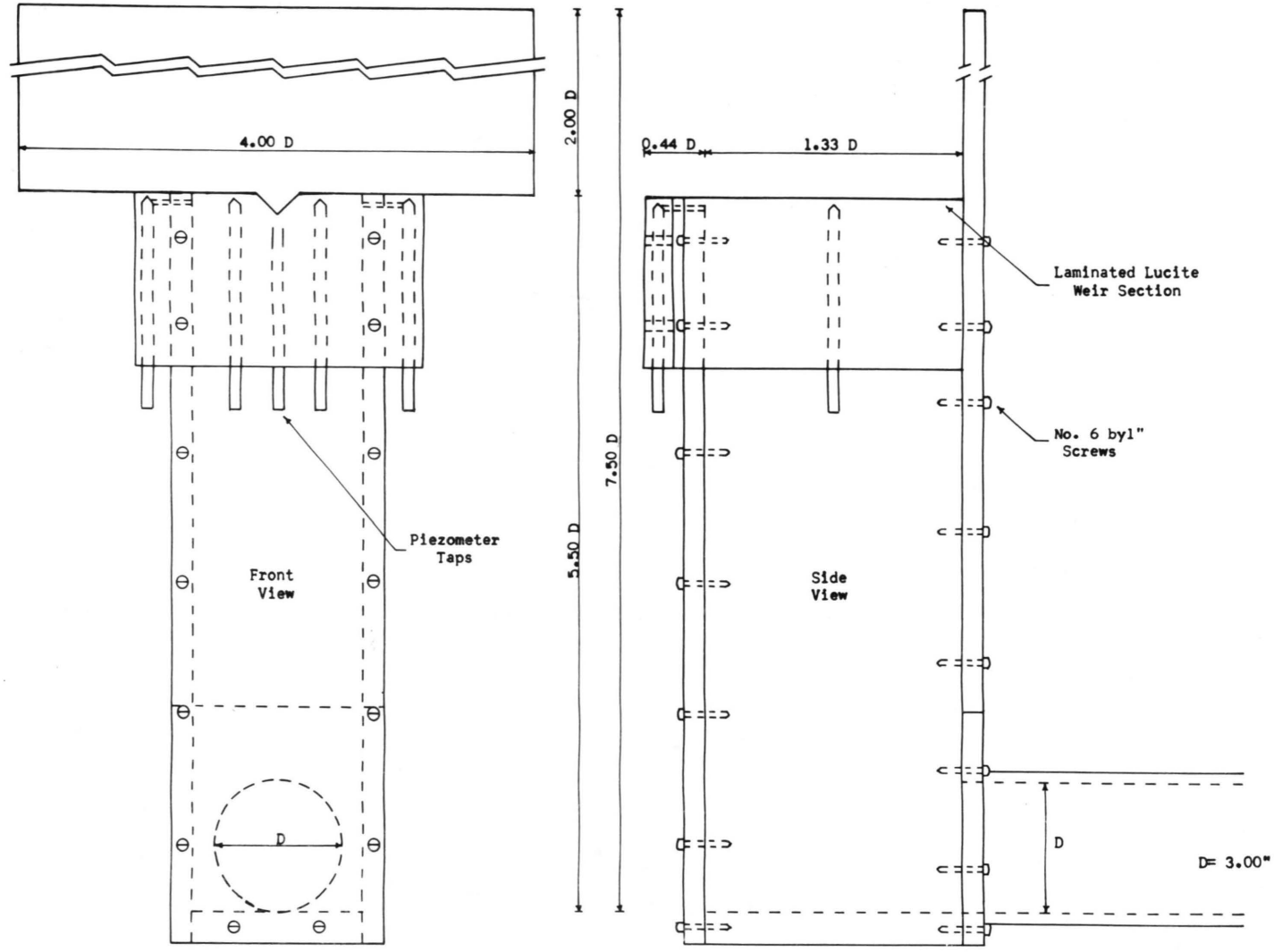

Figure VII. Detailed Drawing of Model Spillway Section

The desired thickness of the weir section of the spillway was 1 and 1/3-inch due to the model to prototype ratio selection of 1:6. It was observed that Lucite sheet thickness dimensions are generally somewhat under the quoted thicknesses. By careful selection of the Lucite material used, a laminated weir section of 1 and 1/3-inches was constructed. An undersized 1/8-inch Lucite section was laminated to an undersized 3/4-inch section which, in turn, was laminated to the body of the spillway. The lamination of the Lucite section was accomplished by chloroform. The weir section can be observed in the photograph of the installed spillway, Figure V.

The spillway was supported in the approach channel tank by two $\frac{1}{2}$-inch Lucite plates which were fastened together with $\frac{1}{4}$-inch by 1 and $\frac{1}{2}$-inch bolts. The top plate was fastened to the spillway by right-angle brackets and number 8 by 1-inch screws. The right-angle brackets were slotted to allow leveling of the spillway weir section after the spillway had been installed in the approach channel tank. All edges were sealed with waterproof automobile body calking compound.

The conduit of the spillway is Lucite pipe having an average inside diameter of 3 inches and an average outside diameter of 3 and $\frac{1}{2}$-inches. The total length of the spillway Lucite pipe conduit was 28 and 1/3-feet. The last 3 and 1/3-feet of the Lucite pipe section was made to simulate corrugated metal pipe. A 12-gauge

galvanized wire was coiled around a 2 and ½-inch, outside diameter, steel pipe. The coiled wire was threaded into the Lucite pipe section, and the coil spacing was adjusted by a trial and error laboratory procedure until the desired friction factor was obtained. Table 1 is the results of the last set of tests obtained from this trial and error procedure. Figure VIII is a photograph of the installed end section.

Couplings between each section of the Lucite conduit were constructed by selecting undersized, 3 and ½-inch, inside diameter, Lucite pipe which was 6 inches long. These sections were then machined to fit the specific 3-inch, Lucite pipe joint. Silicon grease was placed between the conduit and the coupler to seal any air and water leaks. The first 6-inch coupler can be observed in Figure VI.

Table 1. Final Corrugated Metal Simulation Tests

Run number	Pressure loss for 2 feet (ft)	Time (sec)	Q (cfs)	f_c	Wire spacing changed
1	0.2377	17.3	0.2315	0.0860	
2	0.2500	17.0	0.2355	0.0874	
3	0.2500	17.7	0.2125	0.0948	
					X
4	0.1625	18.2	0.2200	0.0653	
5	0.1500	18.0	0.2222	0.0590	
6	0.1500	17.8	0.2245	0.0579	
					X
7	0.1667	17.9	0.2235	0.0656	
8	0.1708	17.6	0.2275	0.0639	
9	------	17.6	------	------	
					X
10	0.2460	18.0	0.2222	0.0965	
11	0.2500	17.6	0.2275	0.0935	
					X
12	0.2500	18.1	0.2210	0.0989	
13	0.2835	17.0	0.2355	0.0992	
14	0.3080	16.3	0.2455	0.0992	
15	0.3333	15.7	0.2550	0.0992	
16	0.3667	15.3	0.2610	0.1042	
17	0.3000	17.6	0.2272	0.1125	
					X
18	0.2291	17.5	0.2285	0.0856	
19	0.2330	16.8	0.2360	0.0811	
20	0.2375	16.6	0.2410	0.0793	

Table 1. (continued)

Run number	Pressure loss for 2 feet (ft)	Time (sec)	Q (cfs)	f_c	Wire spacing changed
					X
21	0.2400	17.2	0.2325	0.0814	
22	0.2410	16.7	0.2395	0.0812	
23	0.2670	17.0	0.2355	0.0935	
					X
24	0.1750	17.4	0.2300	0.0645	
25	0.1750	17.4	0.2300	0.0645	
26	0.1624	16.8	0.2382	0.0555	
					X
27	0.2500	17.1	0.2340	0.0887	
28	0.2581	17.0	0.2355	0.0904	
					X
29	0.2081	16.7	0.2395	0.0734	
30	0.2040	16.5	0.2425	0.0672	
31	0.2960	14.4	0.2780	0.0743	
32	0.2960	14.3	0.2800	0.0730	
33	0.3000	14.4	0.2780	0.0754	
34	0.2960	14.5	0.2760	0.0755	
35	0.3080	14.6	0.2740	0.0796	
36	0.3045	14.3	0.2800	0.0752	
37	0.3085	14.4	0.2780	0.0776	
38	0.3290	13.9	0.2880	0.0770	
39	0.3125	13.9	0.2880	0.0732	
40	0.3250	13.8	0.2900	0.0729	

This final spacing of approximately 2 and 1/2-inches was used for all flowing tests.

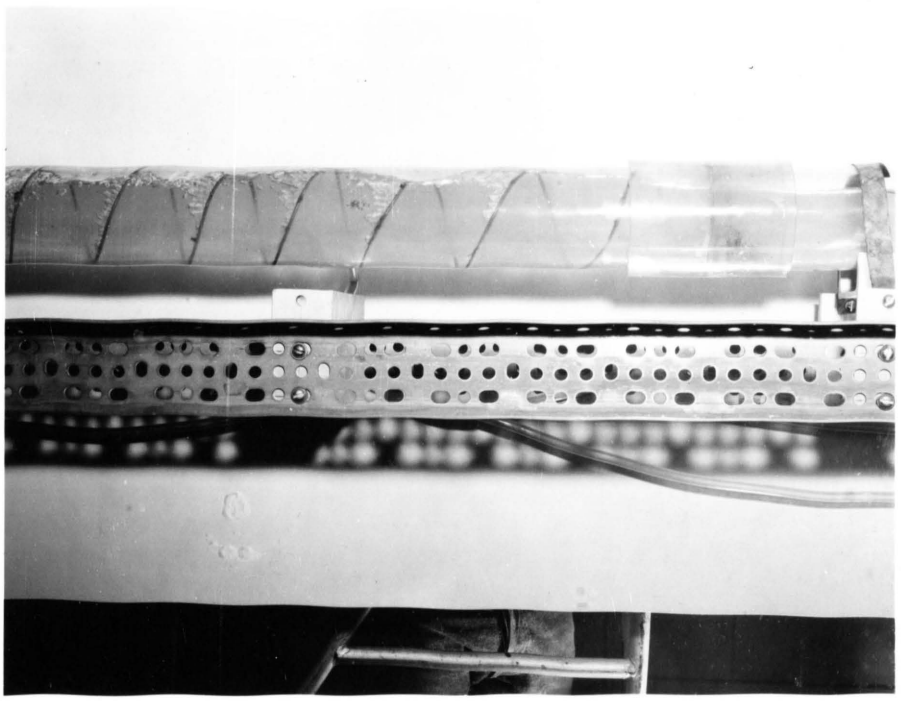

Figure VIII. Simulated Corrugated Metal End Section

Approach Channel

Figure III is a photograph of the hydraulics laboratory test apparatus and shows the approach channel tank. The approach channel was a 16-foot long, number 10 gauge, steel tank. The tank was 5 feet wide and 30 inches deep. The relatively long tank provided excellent simulation for the operation of the spillway with a free water surface such as is found in watershed detention basins, farm ponds, and other artificial reservoir constructions. The tank was supported in the hydraulics laboratory by four 12-inch, 16 pounds per foot I-beams and by four 4-inch, 2.2 pounds per foot, channel hangers. The I-beams were end supported on the laboratory walls. The tank hangers and beams were so spaced so that the tank would settle evenly when filled with water.

Water was supplied by two 3900 g.p.m. turbine pumps and a variable speed centrifugal pump to a constant head tank in the hydraulics laboratory. Water was distributed throughout the laboratory by an 8-inch distribution supply line and subsequently delivered to the approach channel tank by a 6-inch supply line. The spillway flow rate could be regulated by a valve in the 8-inch supply line, a valve in the 6-inch supply line, and a drain valve in the approach channel tank.

All tests were conducted with a 1:3 upstream, simulated, dam embankment (Figure V). The embankment was constructed of 1/8-inch, clear, Lucite sheets.

Spillway Conduit Cradle

The spillway conduit was supported on an existing cradle consisting of two 3-inch aluminum channels with 6-inch aluminum channel spacers approximately 18 inches apart. The existing cradle was extended 12 feet with stamped, Amco steel angles also spaced with the 6-inch aluminum channel spacers 18 inches apart. The original conduit cradle was bolted to an adjustable channel hanger that was fastened to the center tank hanger. The midspan of the existing cradle was supported by an adjustable, overhead, screw jack that raised and lowered the aluminum cradle. The added section of the cradle was supported by two adjustable, pipe and rod hangers supported from the hydraulics laboratory ceiling trusses.

The Lucite conduit was supported on the cradle by 2-inch long, 3-inch slotted, aluminum channels positioned so that the channels were upward, and also by inserting a 3/4-inch plywood spacer between the upward channel and the Lucite conduit. The Lucite conduit was held fast to the cradle by galvanized, light metal U-clamps around the conduit and fastening to the cradle body.

The slope of the cradle was determined and adjusted to the desired slope by setting up a surveyor's level on the hydraulics laboratory floor and inverting the rod to reach the spillway conduit. The desired slope of 1.17 per cent was adjusted to the nearest 0.002 of a foot.

Discharge Collection

The spillway conduit discharge was collected in a 6-inch, flexible, rubber conduit. The rubber conduit discharged into a weighing tank where the spillway conduit discharged was weighed. Free surface conditions existed at the spillway conduit exit at all times. Figure III shows the flexible rubber conduit discharging into the weigh tank.

Discharge Recorder

One channel of the two-channel, Brush oscillograph model, RD23 2100, was used for recording the period of time necessary for 249.6 pounds of discharge from the spillway. An available photoelectric cell circuit was employed to automatically lift the pen of the oscillograph during the given increment of discharge. The chart markings were such that each main chart line space (5mm) represented one second. Therefore, the seconds could be read directly from the recorded chart. Figure IX is a typical discharge recording.

Figure X shows the photoelectric cell unit. A white paper face was placed over the scale face and a black mark over the scale needle. As the tank filled, causing the scale needle and paper to rotate, the black mark on the needle would pass a photo-electric cell which would energize a solenoid and raise the oscillograph pen. When the given increment of water was discharged from the spillway, the black mark would pass another photoelectric

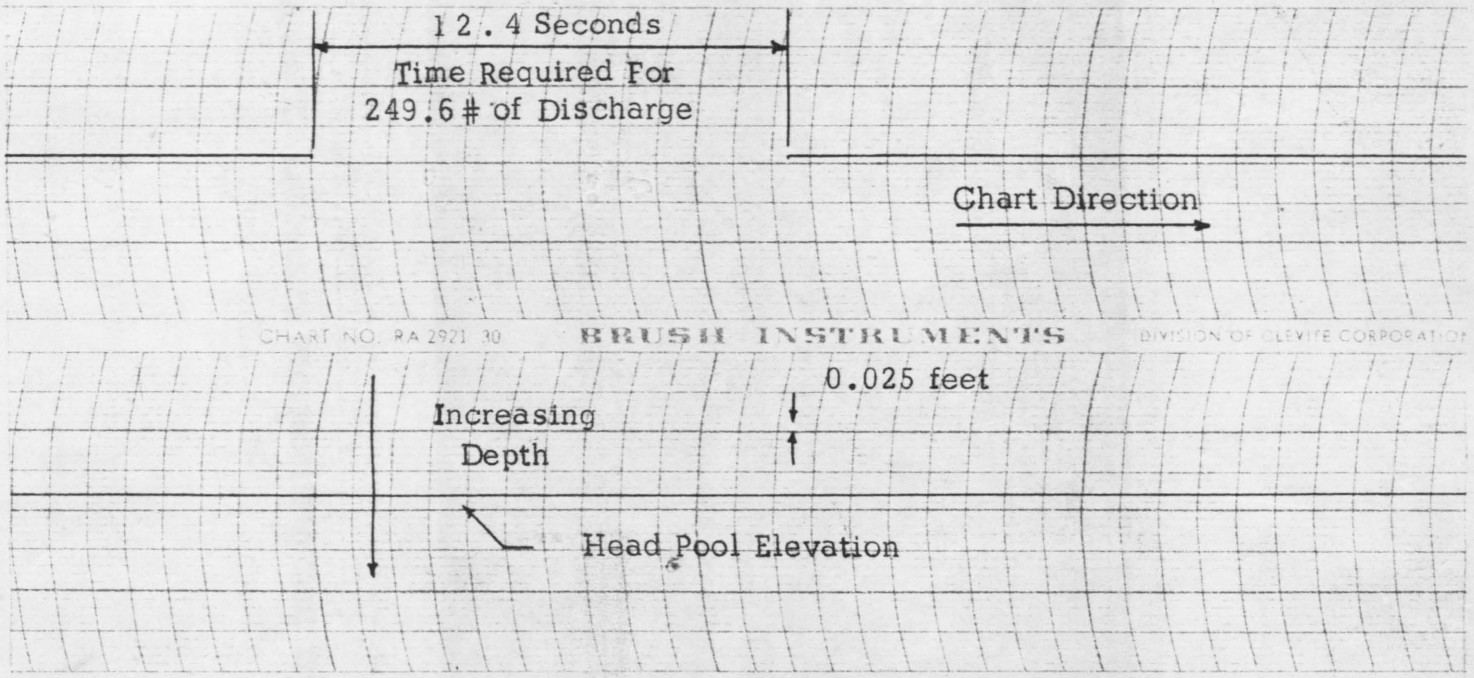

Figure IX. Typical Laboratory Discharge and Head Pool Elevation

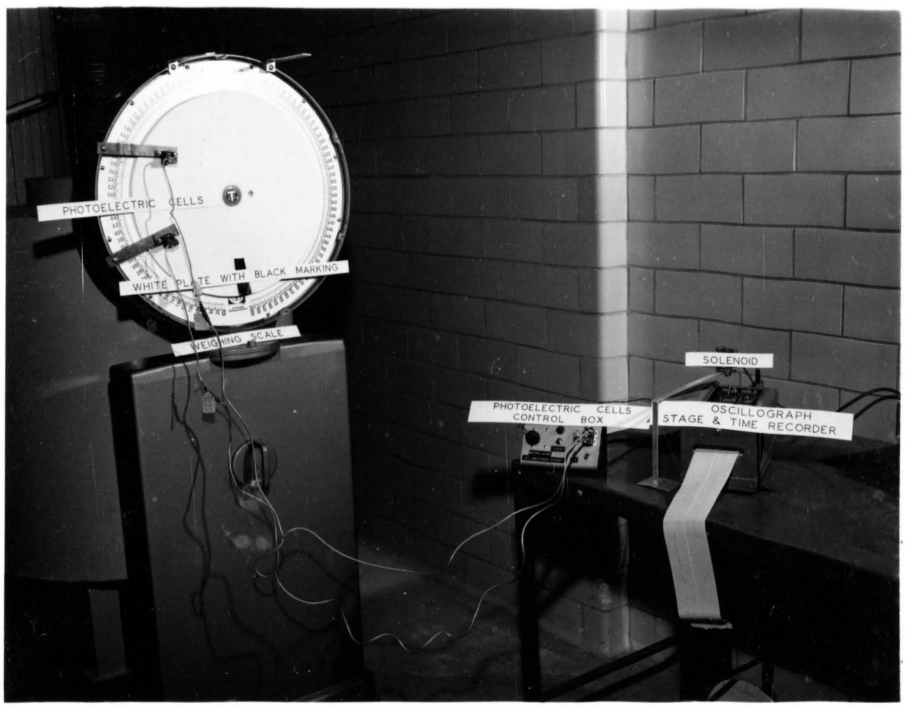

Figure X. Laboratory Photoelectric Cell Timing Unit

cell that would deenergize the solenoid and lower the oscillograph pen. A detailed drawing of the photoelectric cell circuit is found in Figure XXV.

Stage Recorder

The continuous stage was recorded by a combination of the available instrumentation. Figure XI is a photograph of the instrumentation used to record continuous stage. The basic principle employed is that the flow of current through a Wheatstone bridge circuit depends on the amount of unbalance of the Wheatstone bridge circuit. A synchro system was employed to drive a ten-turn variable resistor in one leg of the Wheatstone bridge circuit which was connected to a model, RD56 1200, Brush amplifier and a model, RD23 2100, two-channel, Brush oscillograph. Various full-scale deflections (6, 12, and 24 inches) were employed by changing the Brush amplifier multiplier. The oscillograph used has a relatively fast chart speed (5mm per second) which allowed the recording of small fluctuations in the approach channel water elevation. The basic circuit diagram for the stage recorder is given in Figure XXIV.

The synchro system used to drive the variable resistor is a portion of the Shand and Jurs Company's remote reading tank gauge, model 6245. The synchromotor was removed from the original dial mechanism of the gauge, and a frame was constructed to position the synchromotor. The synchromotor was attached to the variable resistor with a 1-inch, hard-rubber, flexible shaft. The basic

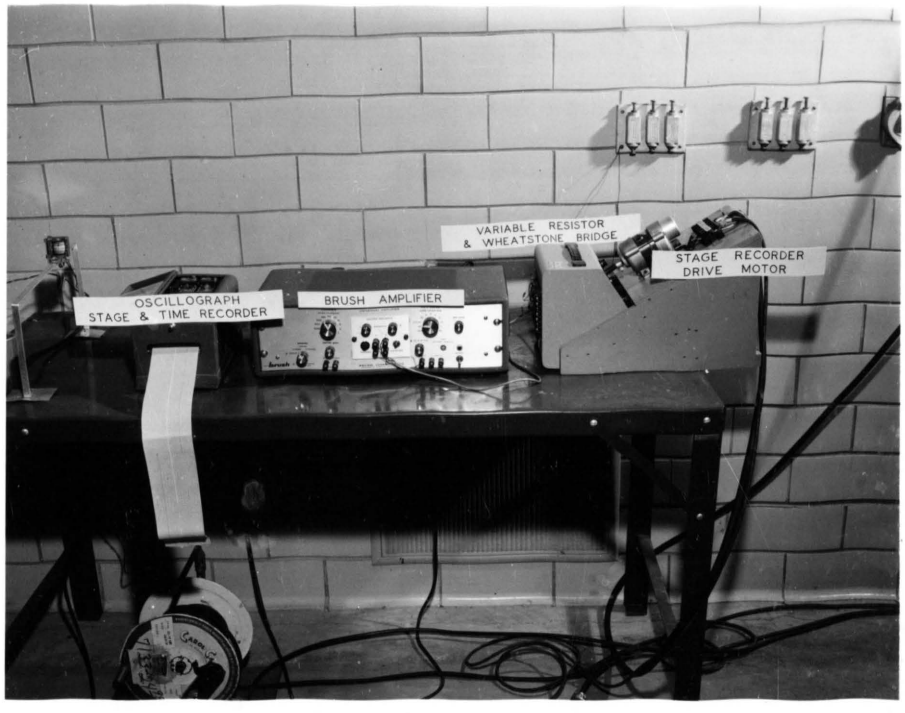

Figure XI. Instrumentation for Laboratory Discharge Recording

circuit diagram for the synchro system is given in Figure XXVI.

A hook gauge was also employed to record water elevation of the approach channel. The hook gauge was employed in order to obtain stage recordings to 0.001 of a foot which could not be accomplished with the continuous recording instruments. Figure XII shows the synchrogenerator and the hook gauge installed in the approach channel tank.

Figure IX is a typical approach channel elevation and discharge recording.

Differential Manometer

Piezometer taps were located at intervals along the bottom of the Lucite conduit and at various points on the spillway to determine pressures and to evaluate the piezometric grade lines. A line was scribed on each section of the conduit, and the piezometer taps were located on these lines. When the spillway was assembled, the scribed piezometer lines were located slightly off the bottom to eliminate obstruction of the taps by any foreign material that was in the water. Figure VI shows the location of tap number 7 on the spillway and tap number 8 on the conduit. Figure VII shows the location and construction of the five piezometer taps (number 1-5) on the lip of the spillway.

The piezometer taps were constructed by drilling a 1/8-inch hole through the Lucite material and securing, with chloroform, a $\frac{1}{4}$-inch countersunk hole in the Lucite. Soft, plyable, $\frac{1}{4}$-inch ,

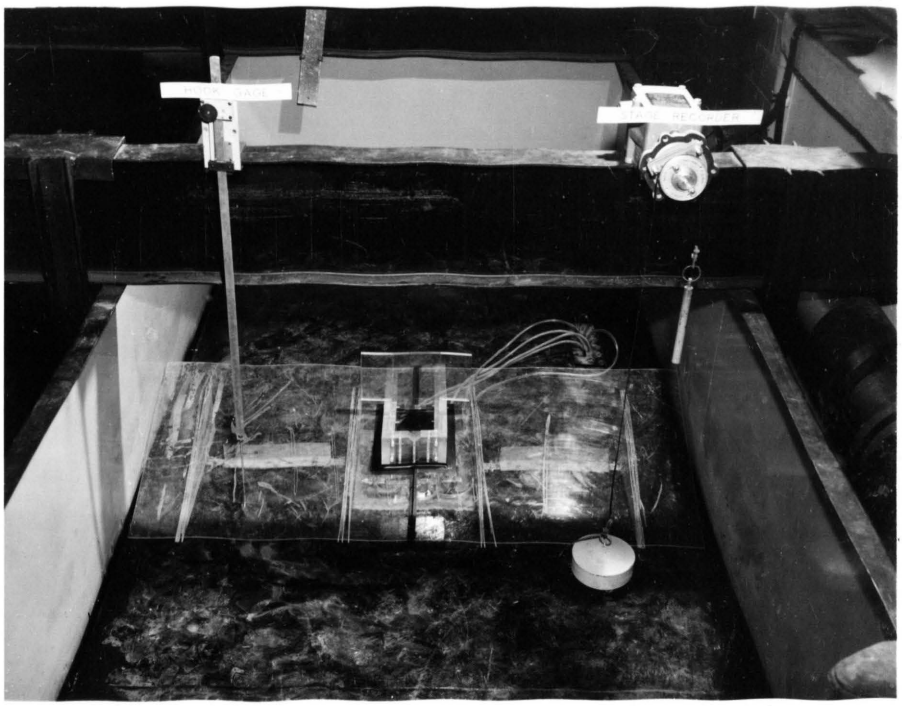

Figure XII. Stage Recorders for Approach Channel

inside diameter, plastic tubing was used to attach the piezometer taps to the manometer board. Figure XIII shows the location of all taps on the entire model.

The pressures were measured by an open-air well, 15-tube, manometer board. The manometer board was originally designed to measure negative pressure and was converted to measure positive pressure relative to the well. The well was attached to a reference manometer by means of a constructed T-system. A valve was also inserted at the T-connection so that the part of the system that contained the manometer fluid could be evacuated of any air that was introduced during filling. All manometer markings are scribed on 0.1 inch intervals. The first 83 runs were performed with a prepared manometer fluid with the specific gravity of 2.00. Due to bad tube connection, the manometer fluid was lost, and the rest of the runs were made with a prepared manometer fluid with the specific gravity of 1.75. Figure XIV is a photograph of the manometer board in operation.

The datum plane of the manometer board was established by running a set of levels with a surveyor's level from the spillway lip to a specific elevation on the manometer board.

Piezometer Tap Number	Distance From Spillway
1 - 7	Spillway
8	0.33D
9	16.33D
10	32.33D
11	64.33D
12	80.33D
13	96.33D
14	101.00D
15	104.33D

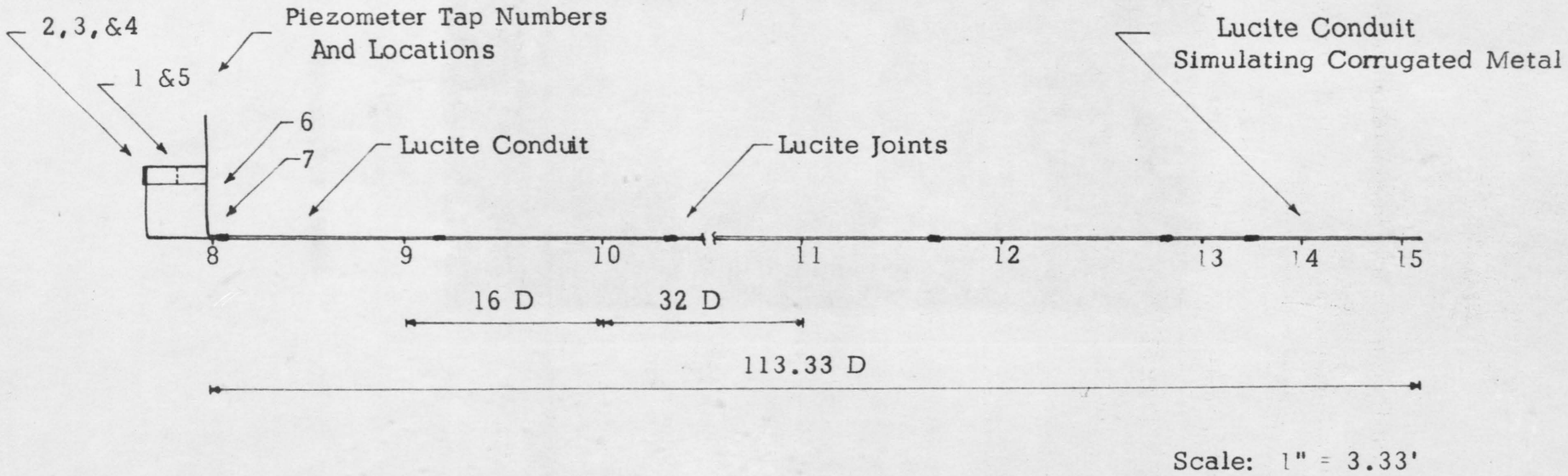

Figure XIII. Piezometer Tap Locations

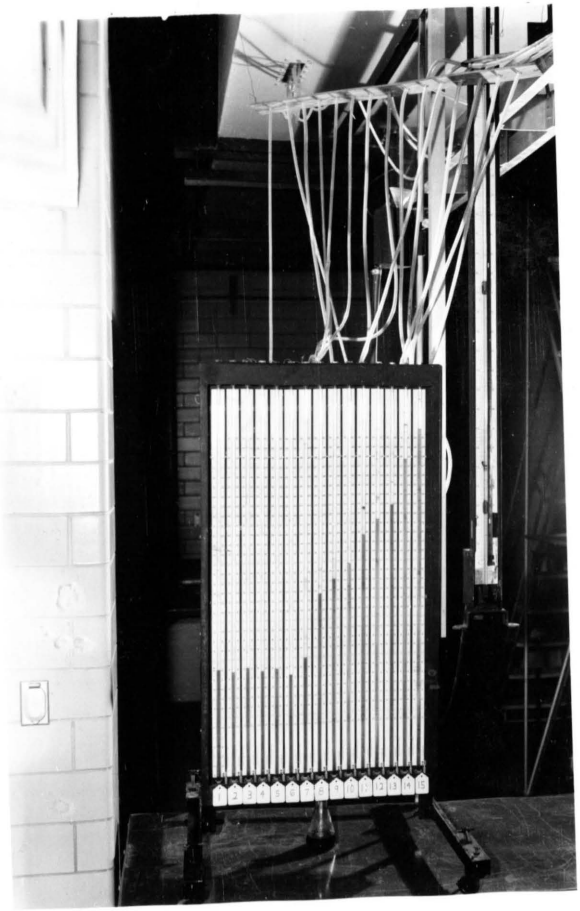

Figure XIV. Manometer Board

LABORATORY TEST PROCEDURE

The laboratory testing procedure combined methods previously used for collection of similar data with improvements imposed where it was felt greater control or ease of operation were required.

Personnel Requirement

The laboratory apparatus and instrumentation was originally designed so that one person could collect all necessary laboratory data. The original instrumentation design employed photographic equipment in conjunction with the previously described instrumentation to simultaneously record the manometer data for each specific run. Since it was impossible to obtain the necessary photographic equipment at the time testing was to be initiated, the testing was begun without the photographic equipment. It was found that the fluctuation of the manometer fluid was not excessive, and the added expense for photographic procedures did not warrant the slight increase in accuracy that would be obtained. Therefore, it became necessary to employ two people to record all necessary data developments and observe the general spillway operation. The following discussion describes the particular responsibility of each observer.

Data Collection

The ordinary procedure in collecting data of this nature is to set a rate of flow, wait until headpool stabilization occurs, and

then make all needed observations. For low flows this procedure is satisfactory, but for higher flows, especially full-pipe flow, this procedure requires relatively long periods of elasped time between each observation. Therefore, for almost all flows, data was collected with an unstable headpool over a relatively short period of time (12-16 seconds). The direction of change in headpool elevation was recorded to evaluate the effect of this procedure. Also, periodically the headpool was allowed to stabilize, and observations were obtained under stable headpool conditions.

Testing was initiated by filling the headpool tank and then closing the supply line valve and allowing the headpool elevation to stabilize at the spillway lip elevation. The supply line was then incrementally opened, and successive collection of data was obtained over the desired headpool elevation range. Each run was initiated by presenting the photoelectric timing unit and then closing the weigh tank discharge valve, retaining all the conduit discharge in the weigh tank. The scale needle would then rotate, and the photoelectric timing unit would automatically record the time for a given increment of discharge. When approximately one-half of this increment was discharged, the headpool elevation was read on the hook gauge and recorded. A Fahrenheit thermometer was attached to the hook gauge, and periodic temperature readings were obtained. The valve on the weigh tank was then released and the water allowed to discharge into the hydraulics lab supply, preparing the system for

the next run. Also during this increment of discharge, the 15-tube manometer board and the manometer board reference were read and recorded. The continuous stage recorder was also in operation during this increment of discharge, and any excessive fluctuation of the headpool elevation could be detected and the run rejected when this occurred. Since the relative cross section of the headpool tank was large, fluctuation of the headpool was slight, and no runs were rejected because of excessive fluctuation. The headpool tank discharge value was used in some cases to obtain desired headpool elevation in the transition region from weir flow to pipe flow. The data was collected with one person performing the manipulation of the equipment and recording the headpool elevation and temperature. Both persons were employed in observing the general operation of the spillway and recorded any pertinent information for future evaluation.

It is estimated that the average time required to obtain the data for one complete run was three minutes. This included resetting of the instrumentation and preparing the system for the next run. If all realms of the model data collection were not completely satisfactory, the run was rejected and another run in the same general area obtained. The testing was initiated at very low flows and proceded at an interval of approximately 0.01 foot increase in head above the spillway lip until 1.3 feet above the lip was reached. At this point, the data collection was terminated because the permissible head in the headpool tank was reached, and also the

model spillway was performing well up into the full-pipe flow range. When it became necessary to discontinue the data collection during the testing, the starting head for continuing the data collection was always well below the discontinue head to eliminate any adverse effect due to discontinuence.

Detailed information and figures concerning the construction and operation of the instrumentation employed in obtaining the data are discussed in the "Laboratory Apparatus" section.

LABORATORY ANALYSIS

Stage and Discharge Recordings

Two-hundred and ninety runs up to an elevation of 1.30 feet above the lip of the model spillway were recorded and analyzed. The continuous synchro-oscillograph stage recorder recorded the elevation of the headpool and any fluctuation in the headpool elevation. The lower half of the oscillograph recording indicated the headpool elevation. The full-scale deflection of the discharge half of the recording was adjusted by the carrier gain of the Brush amplifier depending on the estimated range of elevation change during a specific period of testing (refer to Discharge Recorder, "Laboratory Apparatus" section). Figure IX is a typical oscillograph recording of elevation and time with the full-scale deflection of the elevation recordings set at one foot. The time recorded for the desired increment of discharge was read from the oscillograph recording, and the discharge was determined in the laboratory. Each oscillograph recording was marked with its respective run number with a grease pencil to facilitate chacking of the data.

Manometers

The 15-tube manometer board was read directly during the interval that the time was being recorded for an increment of discharge. Table 2 is a random sample of the recorded manometer

Table 2. Random Sample of Laboratory Data

Run No.	* t	h	Piz. Ref.	Piezometer tap Numbers 1	2	3	4	5	6	7	8	9	10	11	12	13	14	15
84	16.50	0.192	52.75	----	----	----	----	----	3.40	4.86	9.70	10.10	12.3	15.2	17.85	18.4	23.3	25.85
108	15.50	0.420	53.40	----	----	----	0.20	0.20	0.4	1.50	10.60	11.45	13.40	16.7	18.60	20.40	26.15	28.95
151	14.75	0.618	54.95	0.50	----	----	0.30	0.40	0.85	1.35	11.00	12.15	14.20	17.95	20.00	21.90	28.60	31.50
211	13.85	0.909	56.85	2.50	----	----	2.40	2.30	2.80	0.35	10.90	11.80	14.20	18.90	26.70	22.80	30.70	33.90
244	13.40	1.092	59.50	1.90	2.10	2.30	2.20	2.00	1.40	4.10	15.20	16.60	19.10	23.30	25.70	27.90	-----	-----
254	12.85	1.290	60.65	0.20	0.80	0.50	0.50	0.30	0.35	2.70	15.30	16.60	19.40	23.90	26.70	29.00	-----	-----
264	13.05	1.227	60.65	1.10	1.30	1.30	1.20	1.20	0.50	3.5	16.30	16.90	19.80	24.20	26.80	29.25	-----	-----
277	14.90	0.570	56.35	1.20	1.30	1.40	1.40	1.20	0.80	2.90	12.40	13.35	15.50	19.00	21.10	22.90	29.5	32.45

data, and Figure XIII gives the specific location of these taps on the model. For the first 84 runs, pressure loss between each successive piezometer tap could be read directly from the difference between the elevation of the fluid which had a specific gravity of 2.00. Due to a break in a manometer line, the fluid was lost, and a new, less expensive fluid with specific gravity of 1.75 was substituted. Therefore, on the remainder of the tests the difference between the manometer tubes had to be converted to water pressure by multiplying by 0.75. Due to the limited number of manometer tubes on the available board, a manometer was not used to determine the free water surface relative pressure, and it had to be calculated using the relative elevations determined in the laboratory. Table 3 is a summary of the relative elevations in the laboratory.

Because negative pressures due to acceleration were recorded on almost all of the riser section, a combination coefficient of head loss (K_r) was determined, including the riser and transition loss into the conduit. The Darcy-Weisbach friction factor, f_f, was determined for the relatively smooth conduit and f_c for the end section which simulated a corrugated metal section. A coefficient of head loss (K_t) was determined for the transition from the relatively smooth conduit to the rough conduit. A discharge rating equation was derived with the Bernoulli equation, using the calculated coefficients and friction factors. The calculated

Table 3. Relative Elevations of Specific Model Locations

Locations	Elevations
0.00 Man. Board	0.000
Weir Lip	7.254
Piz. taps, 1-5	7.233
Piz. tap 6	6.473
Piz. tap 7	6.181
Piz. tap 8	5.899
Outlet Pipe Bottom	5.860
Piz. tap 9	5.853
Piz. tap 10	5.806
Piz. tap 11	5.712
Piz. tap 12	5.665
Piz. tap 13	5.619
Piz. tap 14	5.596
Piz. tap 15	5.573

equation followed the recorded model discharge data within 3 per cent. Table 4 gives the loss coefficients, and the friction factor for the manometer data given in Table 3. All symbols used in the foregoing tables are defined in Appendix A. The Reynolds number (R_e) was also calculated to indicate the region in which the flow in the conduit was occurring.

Appendix B gives some sample calculations of these dimensional constants and the method of analyzing the data.

Table 4. Typical Loss Coefficients and Reynolds Numbers

Run No.	h_m	Q_m	V_m	K	f	K_t	f_c	Temp. (°F.)	$R_e \times 10^5$
84	0.192	0.2420	4.93	1.04	0.0156	0.390	0.0530	68.5	1.185
108	0.420	0.2581	5.27	1.31	0.0148	0.571	0.0508	69.0	1.279
151	0.618	0.2709	5.51	1.27	0.0148	0.630	0.0478	71.5	1.384
211	0.909	0.2890	5.89	1.31	0.0143	0.673	0.0476	75.0	1.521
244	1.092	0.2985	6.09	1.31	0.0141	-----	------	74.0	1.562
254	1.290	0.3110	6.33	1.27	0.0143	-----	------	74.0	1.623
264	1.227	0.3063	6.25	1.32	0.0139	-----	------	74.0	1.603
277	0.570	0.2685	5.47	1.29	0.0147	0.628	0.0495	74.0	1.403

FIELD APPARATUS AND TESTING PROCEDURE

Description and Location of the Watershed

The Scott Creek is a western tributary of the Big Sioux River and is located in Union County, South Dakota, approximately four miles south and four miles east of the city of Alcester. The watershed has an area of 2,900 acres of which 1,800 are cultivated, 907 acres are grassland, 19 acres woodland and shelterbelt, 39 acres farmstead, and 55 acres roads. The topography is divided into two main divisions, consisting of sharp hills with slopes up to 25 per cent in the central and western parts and the flat benchland in the eastern part lying adjacent to the Big Sioux River.

The detention basin number eleven where all the field data was obtained is in the central portion of the watershed near the change in topography from hills to the flat benchland of the Big Sioux River. The detention basin is reached from Alcester by driving 2 and ¼ miles south, thence left (east) 4 miles, thence right (south) 1 mile, thence east 0.3 miles to gate on the right leading into a pasture where the detention basin and gauges are located, some 0.6 miles from the gate.

Discharge Structure

The mechanical spillway on detention basin number eleven is a typical closed conduit spillway with a circular conduit to divert the excess runoff through the earth dam. Figure XV is a detailed

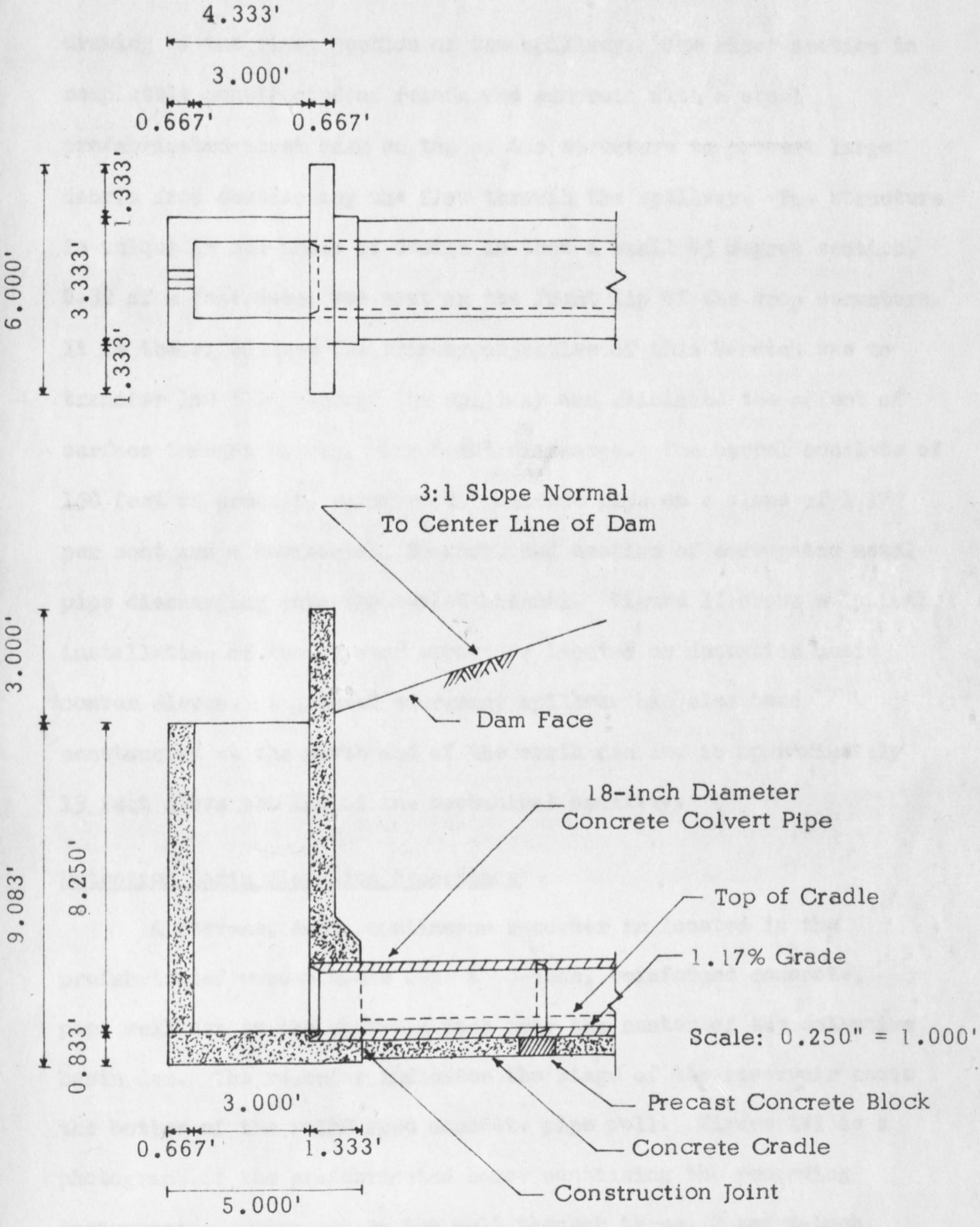

Figure XV. Detailed Drawing of the Field Riser Section

drawing of the riser section of the spillway. The riser section is completely constructed of reinforced concrete with a steel prefabricated trash rack on top of the structure to prevent large debris from obstructing the flow through the spillway. The structure is unique in one phase of design in that a small 45 degree section, 0.32 of a foot deep, was cast in the front lip of the drop structure. It is theorized that the primary objective of this V-notch was to transfer low flow through the spillway and eliminate the effect of surface tension on very "low-head" discharge. The barrel consists of 150 feet of precast, reinforced, concrete pipe on a slope of 1.17 per cent and a horizontal, 20-foot, end section of corrugated metal pipe discharging into the outlet channel. Figure II shows a typical installation of the type of structure located on detention basin number eleven. A grassed emergency spillway has also been constructed at the north end of the earth dam and is approximately 13 feet above the lip of the mechanical spillway.

Detention Basin Elevation Recordings

A Stevens, A-35, continuous recorder is located in the prefabricated wooden house over a 48-inch, reinforced concrete, pipe well set in the upstream face near the center of the detention basin dam. The recorder indicates the stage of the reservoir above the bottom of the reinforced concrete pipe well. Figure XVI is a photograph of the prefabricated house containing the recording instruments. Water enters the well through three, 2 and $\frac{1}{2}$-inch,

Figure XVI. Prefabricated House Containing Stage Recorder

intake pipes with elevations, with respect to the bottom of the well of the bottom of the pipes at 1.75, 3.79, and 5.38 feet respectively. There is a standard flushing system using three-way clocks connecting to each of the intakes to facilitate cleaning.

Elevations of pertinent features are:

1. Bottom of well, 0.00 feet.
2. Lip of spillway, 5.04 feet.
3. Top of frost floor, 7.40 feet.
4. Top of main house floor, 20.16 feet.
5. Top of recorder shelf, 23.31 feet.

The inside gauge is a vertical staff attached to a 2 by 6 plank on the inside wall of the well extended from 0.00 to 19.02 feet. The inside tape gauge is an integral part of the recorder, with an index attached to the recorder shelf. The recorder was set to read the same as the inside staff gauge, and this gauge was used as the reference gauge. The outside gauge consists of vertical staff plates in five sections. The two lower sections, 3.4 and 6.7, and 6.7 to 10.1 feet, are attached to 4 by 6-inch planks fastened to the trash rack of the intake structure. The remaining sections are two planks attached to posts driven in the upstream face of the dam between the gauge and the intake structure. The top outside gauge can be observed in Figure XVI. All gauges described above are set to the same datum.

The recorder is a standard, Stevens, A-35, continuous recorder with a weight-driven time mechanism. The recorder is set with a chart speed of 4.8 inches per day. One inch of travel of the recording pen indicates 0.5 feet of elevation change. If more than five feet of change occurs, the pen automatically reverses itself, and continuous elevation recordings can be obtained for any pond elevation. This recorder has also attached to it a continuous recording, tripping bucket, rain gauge, and the elevation pen is adjusted about 0.3 inches into the upper chart margin to allow operation of the rain gauge pen. Figure XVII is the continuous pond elevation recording for March 26 and 27, 1962, and Figure XVIII is the corresponding Parshall flume recording.

The instruments recording the pond elevation are property of the United States Department of the Interior, Geological Survey. The Geological Survey has allowed South Dakota State College to use these facilities since their discontinuance of data collection in December, 1958.

Discharge Recordings

The discharge was recorded in the discharge channel approximately 100 feet downstream from the spillway conduit by a Parshall flume. The Parshall flume, which was loaned for this project from the Geological Survey at Pierre, South Dakota, has a 36-inch throat width, a 24-inch depth, and a recordable carrying capacity of 28.82 cfs. The flume was installed in the channel on

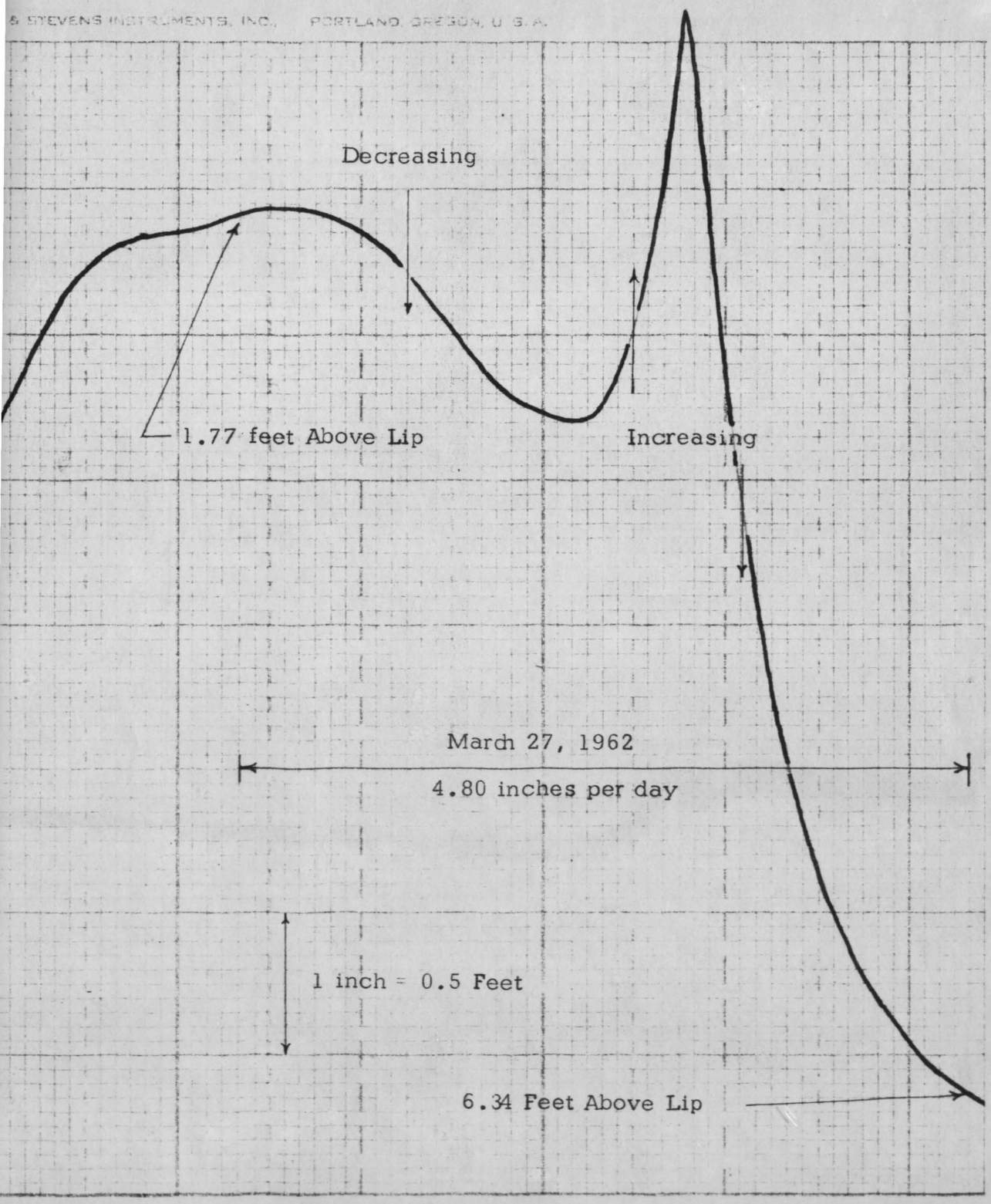

Figure XVII. Typical Continuous Detention Basin Stage Recording

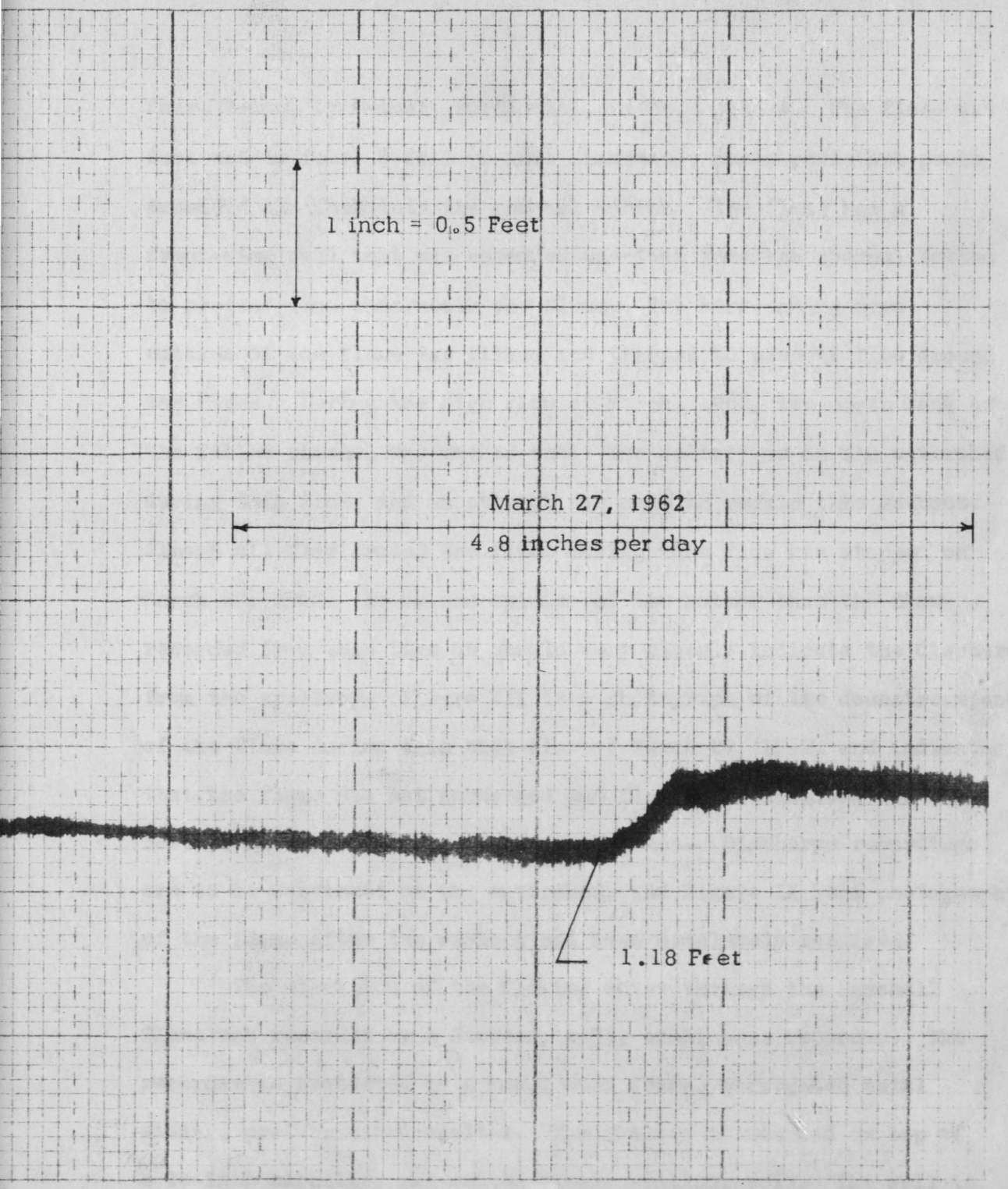

Figure XVIII. Typical Continuous Field Discharge Recording on Parshall Flume

four, 4-inch by 6-inch, horizontal, redwood planks. The flume was fastened to four, 8-foot (6-inch diameter), decay-resistant posts embedded six feet into the channel bottom. The flume has a front-wing wall that was embedded one foot into the channel bottom to prevent flow underneath the flume. The surrounding area outside of the flume was filled and tramped to prevent flow around the flume. During the high flow of March, 1962, the north bank of the filled channel was washed out. The author was on the watershed during this flow, and an attempt was made to repair this washout. Almost all flow around the flume during this flow was stopped on March 29, 1962. It is the opinion of the author that the flow recorded from this time on should very closely indicate the discharge from the spillway. Figure XIX is a photograph of the downstream end of the flume during this high flow of March 29, 1962, and indicates that the flume was not submerged and flow determinations did not have to be corrected for flume submergence. Discharge recordings are to be continued on the watershed, and Figure XX is a photograph of the flume after the washout had been completely repaired.

The elevation of the flowing water through the Parshall flume was recorded by a Stevens, A-35, continuous recorder. The recorder is protected by a small wood frame, corrugated metal siding, prefabricated shelter. The shelter is mounted on top of a 14-inch circular, galvanized steel, stilling well. The well is connected to the Parshall flume by a 3/4-inch pipe. A 12-inch

Figure XIX. Downstream End of Parshall Flume Under Capacity Flow Conditions

Figure XX. Parshall Flume Installed on Watershed

float is contained in the well, and the recording pen is driven by the float and a counter weight. The shelter is also held in place by two, 4-inch, decay-resistant posts imbedded in the channel bank. The shelter can be observed in Figure XX.

The recorder operates the same as the stage recorder. Since there is a very limited distance between the bottom of the shelter and the ground level, some other means than a weight-driven timing and drive mechanism had to be employed. The Geological Survey men had a weight-driven mechanism that they had converted to battery power that was loaned for installing on the recorder. The mechanism was originally designed for two, one and ½-volt batteries with a life expectancy of approximately 15 days. Another set of batteries was installed to increase the required maintenance interval to one month. The recorder was checked for two weeks in the laboratory with the converted mechanism, and it was the opinion of the author that the drive resulted in a constant 4.8 inch travel per day. In analyzing the data obtained from this recorder, it was found that the rate of travel was not constant but would gradually get slower as the batteries decayed, especially in the last week of operation. The author was fortunate enough to be on the watershed during four of the recorded flows, and the author was able to mark both recording charts at that time. The rate of travel of the Parshall flume recorder could then be easily estimated in both directions from this reference.

It was observed that during high flows such as the March, 1962, flow, the field spillway seemed to have a varying flow rate. This varying flow rate is indicated in Figure XVIII by the very wide line on the recorder chart. Figure XVIII is a section of the continuous recording on the flume and corresponds to Figure XVII which indicates the pond elevation over this same period of time. In analyzing the recordings that indicated varying flow of this type, a mean was estimated and recorded as the flow at any given time. It is the opinion of the author that this varying flow is the result of turbulent action caused by the high flow in the relatively short approach channel of the Parshall flume.

All of the field discharge and headpool elevation data was analyzed, employing a time interval of one hour. Under free flowing conditions (unsubmerged), the Parshall flume has been calibrated for different widths of throat (W), and the corresponding equation for determining the discharge (Q) is:

$$Q = 4WH_a^{1.522W^{0.026}}$$

Where:

Q is the discharge (cfs)
W is the throat width (3 feet)
H_a is the head in feet through the flume at a specified cross section

To facilitate determining the field discharge, a table of H_a versus Q for various Parshall flume widths was employed (11).

RESULTS

The primary objectives of this investigation were to determine a field rating curve for the specific spillway and to compare field and laboratory investigations of the spillway. Analysis of data was performed separately, and field, laboratory, and theoretical comparisons were accomplished graphically. Typical data and analysis are found in the respective analysis section.

Rating Curve

Figure XXI is a graphical summarization of the model data obtained. The plotted points on this figure represent the stage-discharge data obtained in the laboratory. The laboratory values were converted to prototype predictions with respect to the Froude law, model-design criteria previously discussed.

By employing the pressure data obtained in the laboratory, the following average model-loss coefficients were determined:

Riser and elbow loss,	$K_r = 1.15$
Lucite pipe friction factor,	$f_l = 0.0145$
Corrugated metal pipe entrance loss,	$K_t = 0.600$
Corrugated metal pipe friction factor,	$f_c = 0.0500$

Analysis methods of pressure data is given in the previous "Laboratory Analysis" section, and sample calculations are given in Appendix B. With these loss coefficients and the Bernoulli equation, a full-pipe flow discharge equation for the model can be derived as follows:

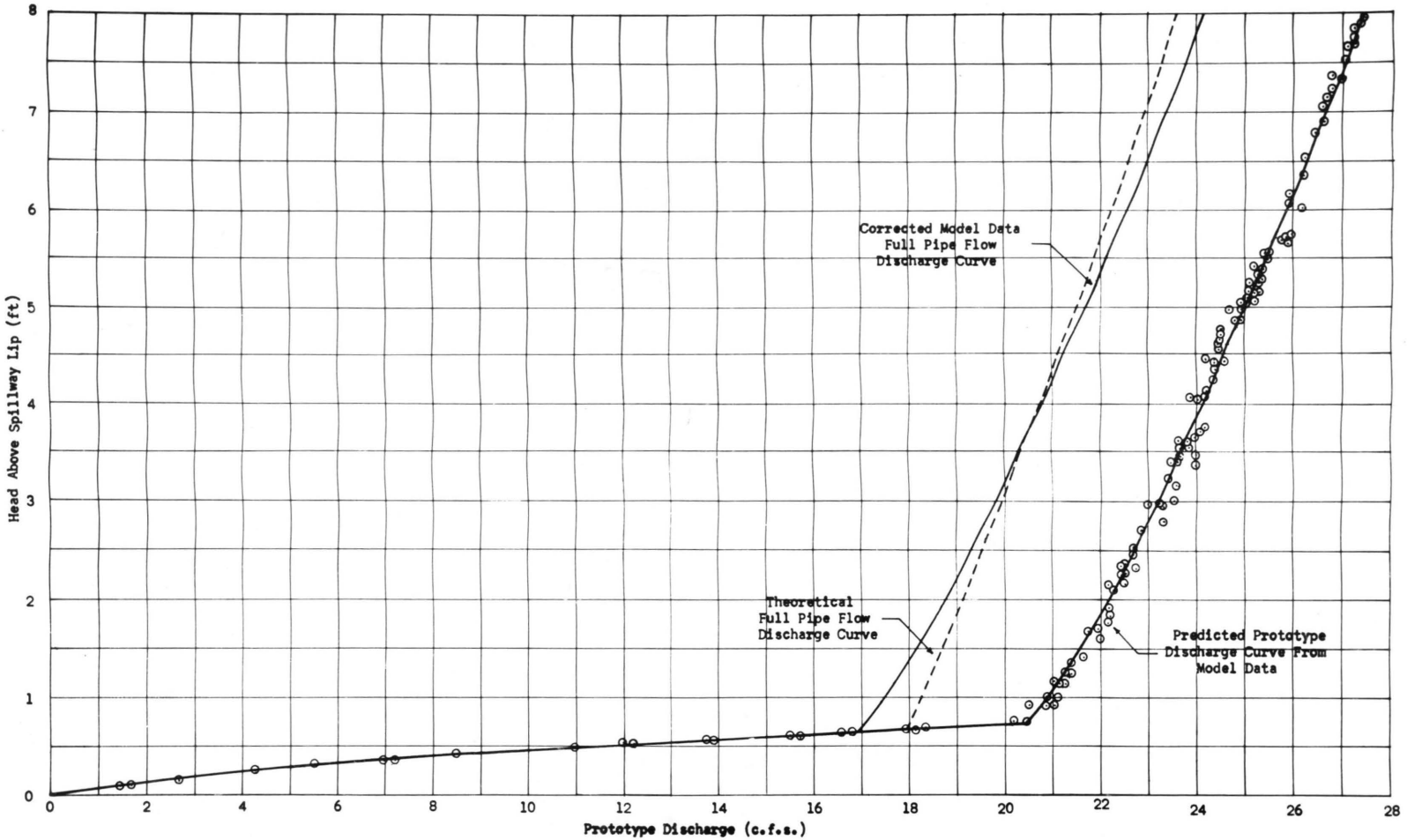

Figure XXI. Predicted Rating Curve From Model Data

$$\frac{V_o^2}{2g} + \frac{P_o}{\gamma} + H = \frac{V_2^2}{2g} + \frac{P_2}{\gamma} + 0 + h_L$$

Where:

$$h_L = \frac{V^2}{2g}\left[K_r + K_t + f_f\left(\frac{L_f}{D}\right) + f_c\left(\frac{L_c}{D}\right)\right]$$

And:

V_o = Headpool velocity (zero)

P_o = Headpool pressure (zero)

V_2 = Average conduit exit velocity (ft/sec)

P_2 = Conduit exit pressure (zero)

L_f = Length of the Lucite conduit (25 ft)

L_c = Length of simulated, corrugated metal conduit (3 and 1/3 ft)

All other symbols are defined in Appendix A.

And:

$Q = a\,V$

Therefore, the full-pipe flow model discharge equation is:

$$Q = 0.1970\sqrt{H}$$

If the model-prototype Froude relationship is applied to this equation, and it is plotted on Figure XXI, it falls within plus or minus one per cent of the curve predicted from the model stage-discharge data. Therefore, it seemed logical and ethical to adjust the friction factor in the concrete and corrugated metal pipe to more representative values (7). By employing these different values (f_f = 0.25 and f_c = 0.73) and the Bernoulli equation with the

same reasoning as above, the theoretical full-pipe flow discharge curve for the prototype of Figure XXI was derived. The equation for the theoretical full-pipe flow discharge curve is:

$$Q = 5.69\sqrt{H}$$

By observation, it was found that the predicted curve had a somewhat greater slope than the theoretical full-pipe flow curve, and, therefore, the curve derived from the model stage-discharge data was superimposed on the theoretical curve. The final corrected, model data, full-pipe flow, discharge curve was then determined. It is the opinion of the author that this slight deviation of the full-pipe portion of the model rating curve was indicative of this specific spillway, and, therefore, the transfer of this deviation to the prototype was performed. The predicted rating curve from model data follows the general weir flow equation up to approximately 16.5 cfs and then continued to follow the corrected, model data, full-pipe flow, discharge curve indicated in Figure XXI.

From the model data and observation of the model, it was concluded that the simulated, corrugated metal, end section caused the spillway to prematurely flow full, and very little slug flow occurred. Therefore, the spillway rating curve made an abrupt change from weir flow to full-pipe flow. Figure VIII of the simulated corrugated metal section shows this section experiencing some slug flow. Although this section did have some slug flow, the other portion of the spillway conduit still had free water surface flow,

and the slugs in the end section did not effect the spillway rating curve.

Figure XXII is a graphical presentation of the field data obtained. The method of obtaining the data is explained in the "Field Apparatus and Testing Procedure" section. One of the major problems confronted in securing field data was that the channel directly downstream from the spillway is in very poor condition with excessive vegetation problems. Also, the channel is quite wide with very little embankment to prevent excessive flooding of a large area when relatively large flow occurred. Also, to install a Parshall flume with capacity to record high flows, it became necessary to sacrifice accuracy in recording relatively small flows. The other major problem encountered in obtaining the field data was not anticipated. The borrowed timing mechanism for the Stevens, A-35, continuous Parshall flume recorder did not have a constant rate of travel which was previously expected. Therefore, it was necessary to be on the watershed sometime relatively close to a flow in order to synchronize the stage and flow recorders. The author was fortunate to be on the watershed at desirable times. Therefore, the field stage-discharge record was obtained for four relatively large flows.

The four recorded flows are indicated in Figure XXII. The early flow (February 15-16, 1962) recorded occurred due to snow melt, and the channel downstream from the Parshall flume was free

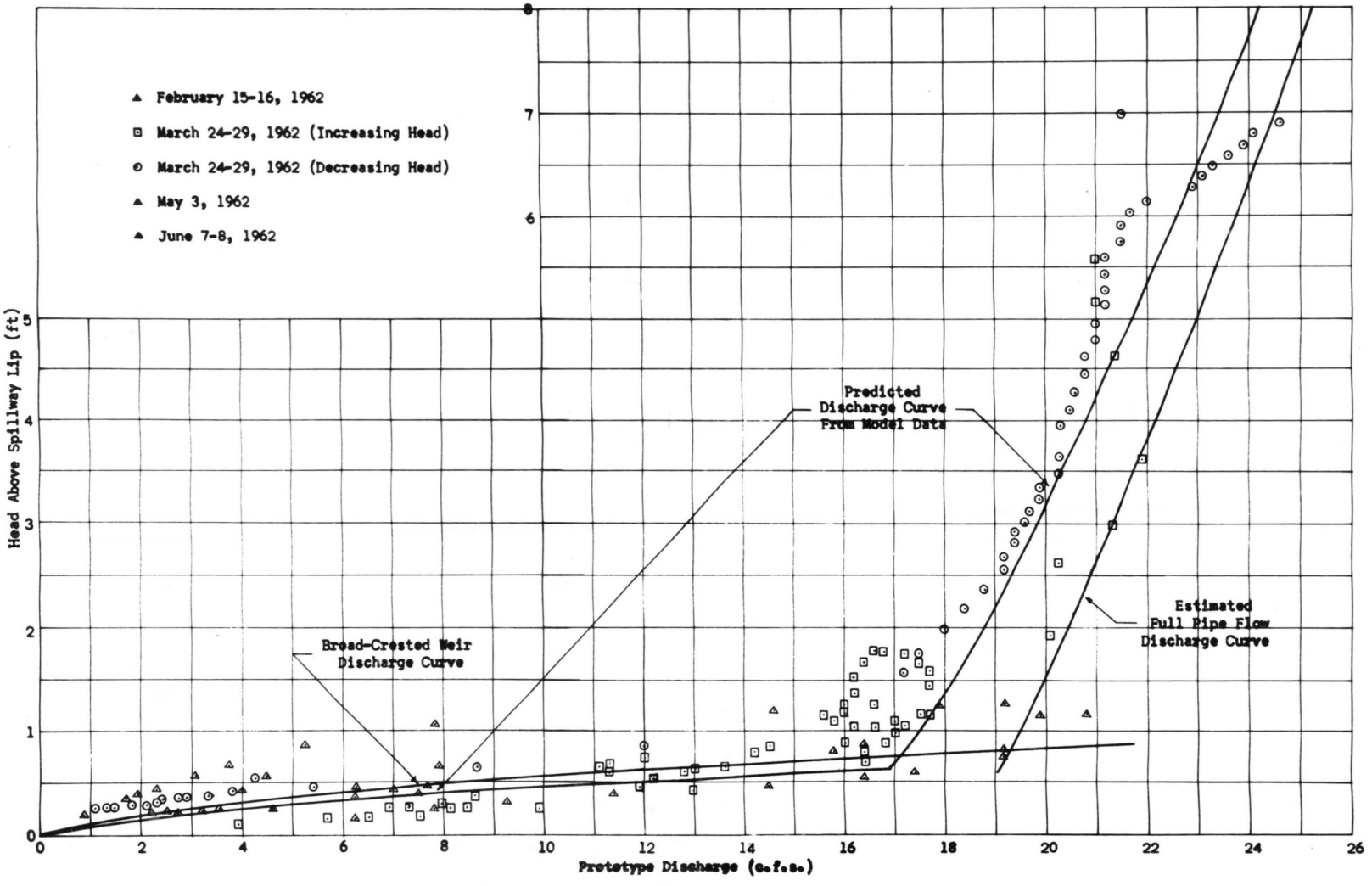

Figure XXII. Theoretical, Laboratory, and Field Rating Curve Comparisons

of vegetation. The Parshall flume was not submerged during this flow, and recordings were obtained up through the high weir flow range. Although these points were not separated from the other weir flow recording, this first recorded flow seemed to follow quite closely to the predicted weir discharge curve from the model data.

The second flow recorded was due to the intense March, 1962, flood which occurred in eastern South Dakota. The excessive high flow resulted in a washout around one side of the Parshall flume. The author was on the watershed on March 29, 1962, the day in which the peak flow occurred through the spillway. We arrived on the detention dam number eleven before noon, and an attempt was made to repair the washout that had occurred. The flow was almost at capacity for the Parshall flume, and the repair material was not too desirable. It was estimated that approximately 95 per cent of the flow was diverted through the flume at this time. Figure XIX is a photograph observing the downstream end of the Parshall flume during this almost capacity flow, indicating that submergence was of no concern during this flow. Figure XX is a photograph of the installed Parshall flume after complete repair work and increased embankment was accomplished. The flume is still installed, and any further high flows of this type should be recorded with more reliable results.

Due to the fact that this washout occurred and the temporary repair work was accomplished, the March, 1962, flow recording was broken into two sections for the graphical presentation of Figure XXII.

Since the repair work was accomplished during peak flow, the early portion was deemed "increasing head" and the portion after the repair work deemed "decreasing head". A portion of the increasing head data was disregarded because it was evident that the washout had occurred during this time, and the recordings were inconclusive. The decreasing head data (indicated by ⓓ on Figure XXII) is well within the range of the model-derived rating curve but does indicate somewhat lesser flow than would be predicted. This would be expected because a small portion of the flow was going around the flume at this time. The increasing head data (indicated by ⊡ on Figure XXII) indicates a few points above the model-derived flow curve. It is surmised by the author that this is due to the excessive vegetation downstream from the flume which had not been removed by the high flow which occurred later.

The other two flows recorded were in the weir flow range. The field data in the weir flow range, with exception of the first recorded flow, seemed to have quite an excessive variance from any definite rating curve. It is surmised that this variance was due to fact that the excessive vegetation downstream from the Parshall flume caused variable submergence of the flume, and, therefore, resulted in inconclusive discharge recording on these relatively low flows. The higher field weir flow recordings seemed to cohere closer to the derived-model weir flow equation, but still no definite trend is obvious from this data.

The theoretical weir discharge curve was derived from the basic equation:

$$Q = CL\ h^{3/2}$$

Considerable discrepency exists in the results of different investigations of coefficients (C) for the broad-crested weir, especially below 0.5 feet. The coefficients used to derive the theoretical weir flow equation vary with the head (h) on the proposed weir. Table 5 summarizes the coefficients used for the theoretical weir flow equation (9) and those coefficients derived from the model data.

Table 5. Broad-crested Weir Coefficients

Head (h) in feet	C	C_m
0.2	2.80	3.90
0.3	2.85	3.88
0.4	2.90	3.90
0.5	2.94	4.02
0.6	2.98	3.87
0.7	3.11	3.92

The flow derived from the basic broad-crested weir flow equation was adjusted by the capacity of the V-notch in the front lip of the spillway to result in the total estimated discharge over the spillway during weir flow conditions. The weir flow equation derived

from the model data indicates higher flow for a given head than the theoretical equation. This could be expected because the lip of the spillway is relatively small in width and has a somewhat curved edge which could vary the nappe characteristics of the spillway and increase the flow for a given head. Although it is generally accepted that the coefficient for the broad-crested weir will increase with depth over the weir (9), the model weir flow discharge curve derived indicated a constant coefficient of approximately 3.90. A summarization of the coefficients (C_m) for different heads on the lip of the spillway derived from the coefficient is over 25 per cent greater than the estimated coefficient. This increase is easily attributed to the variance in the nappe characteristics of this specific weir from the conventional broad-crested weir characteristics.

The estimated full-pipe flow discharge curve of Figure XXII was derived by employing the Bernoulli principle as previously discussed with representative loss coefficients selected from reliable sources (10 and 13).

A combination riser and conduit entrance loss coefficient was estimated to be 1.10. The Darcy-Weisbach friction factor for precast concrete conduit and corrugated metal conduit was estimated as 0.025 and 0.073 respectively. No specific loss coefficient for the transition from relatively smooth to relatively rough pipe was anticipated. Therefore, no attempt was made to estimate a loss at this point. The model investigation later revealed that this

transition results in an important loss and must be included when determining the spillway rating curve.

The equation of the estimated full-pipe flow discharge curve of Figure XXII is:

$$Q = 6.08\sqrt{H}$$

The transition from weir flow to full-pipe flow was quite abrupt and definite in the laboratory. Figure XXI indicates this definite change in flow regime. From the field data, this definite change cannot be detected. The field data varies less than 10 per cent from the model-predicted rating transition, but no definite trend indicating the variance direction can be detected. When this change occurred in the laboratory, the head increased quite rapidly, and it was difficult to obtain data in the transition region. Therefore, in the field it could be expected that the discharge readings would lag the stage readings. Since the field data was analyzed on an hourly basis, a small error in the synchronization of the two recorder timing mechanisms could easily result in a 10 per cent error in the stage-discharge recording in the transition region. In all other regions of flow, the rate of change of the stage discharge was relatively slow, and a small percentage error in the synchronization of the recorders had little effect of the respective stage-discharge recordings.

Spillway Conduit

The field conduit consists of 150 feet of precast concrete pipe laid in a cast concrete cradle and a 20-foot diameter, corrugated metal pipe. In order to select a desirable model to prototype ratio (Model Design section), it was necessary to select a model Lucite conduit size which would not produce simulated roughness between the field concrete conduit and the laboratory Lucite conduit. Although this roughness was not simulated, it is easily assumed by accepted model-prototype design that the final rating curve can be adjusted by assuming a representative roughness for the field conduit. It was found that the 0.25-foot Lucite pipe had a Darcy-Weisbach friction factor of 0.0145. This corresponds to a Manning friction coefficient of n = 0.0107. This indicates about an 11 per cent increase in the laboratory (5). To determine the final model-rating curve for the spillway, the concrete conduit was assumed to have a Darcy-Weisbach friction factor of $f_f = 0.025$ (20).

An attempt was made to simulate the corrugated metal end section in the laboratory. The details of the construction of this section are given in the "Laboratory Apparatus" section. The coiled wire inside of the Lucite conduit was satisfactory to the extent that the roughness was increased to the general range of roughness for corrugated metal conduit. Although the roughness was increased to the general range, it was very difficult to adjust the roughness to a definite constant roughness. A very slight adjustment of the

coiled wire between the piezometer taps could easily change the indicated roughness by as much as 30 per cent. Each coil was not fastened to the Lucite, and the water pressure could change the roughness coefficient as determined by the two piezometer taps located two feet apart on this section. It is surmised by the author that it would be necessary to construct a piezometer tap between each coil and then physically fasten each coil to the Lucite to obtain a definite constant roughness. This procedure is entirely impractical when the roughness can easily be adjusted to the desirable roughness for the final model-predicted rating curve. In the preliminary tests of the simulated, corrugated metal section, the Darcy-Weisbach friction factor was adjusted to the desirable value of $f_c = 0.073$. Although the laboratory apparatus was not altered from this time until the spillway tests were concluded, the corrugated metal section had a friction factor of $f_c = 0.050$. This factor was lower than what would have been most desirable, but the section produced the desirable characteristics of increasing the roughness into the range of corrugated metal conduit and resulted in observance of the operation of a closed conduit spillway with an end section of relatively high roughness.

Since it is desirable to have an equation for the spillway rating curve, Figure XXII-a, Logarithmic Plot of Full-Pipe Flow Rating Curves, was employed. From Figure XXII-a, the predicted full-pipe flow discharged curve from the model data can be derived as

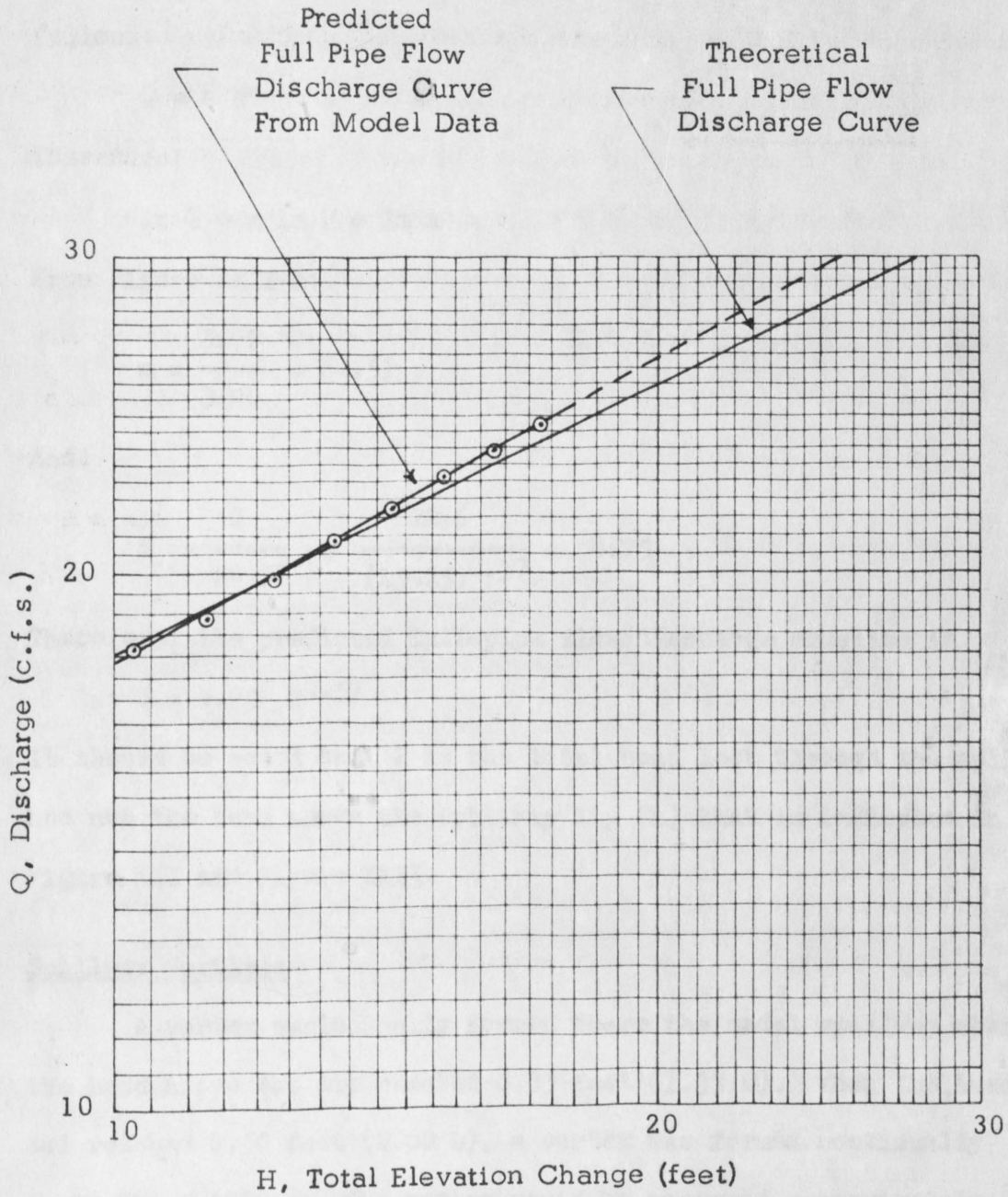

Figure XXII-a. Logarithmic Plot of Full Pipe Flow Rating Curves

follows:

$$Q = A\ H^m$$

Therefore:

$$\ln Q = m \ln H + \ln A$$

From Figure XXII-a:

$$m = \frac{1.70}{3.00} = 0.57$$

And:

$$A = \frac{Q}{H^{0.57}} = \frac{22.6}{(15.25)^{0.57}} = 4.75$$

Therefore, the predicted full-pipe flow discharge equation is:

$$Q = 4.75\ H^{0.57}$$

It should be noted that H is the total head lost through the spillway and not the head above the spillway lip (h) that is indicated in Figure XXI and Figure XXII.

Spillway Vortices

A vortex periodically formed above the model spillway when the head above the lip reached 0.33 feet (1.33 D). When the head had reached 0.50 feet (2.00 D), a vortex was formed continually above the spillway. The vortex could be observed approximately 3/4 of the distance to the bottom of the drop box. At no time could the vortex tail be observed entering the conduit. The vortex formed well up into the full-pipe flow range, and no detrimental effect to the structure or the discharge could be detected.

In observing the field spillway, no vortex could be detected under any flow conditions. The only possible explanation of this discrepancy between the model and prototype is that the model spillway did not have a simulated trash rack constructed on it as the prototype did. It is surmised that the prototype trash rack presented enough disturbance to the spillway flow to disrupt the vortex establishment.

V-notch

The front lip of the field spillway has constructed in it a 45 degree V-notch, 0.32 feet deep. It is assumed that this notch was constructed in the lip to convey with better hydraulic efficiency low flows through the spillway. The maximum capacity for the V-notch is 0.1225 cfs. The V-notch was also constructed in the model to simulate the prototype. An attempt was made to investigate the discharge characteristics of the V-notch, and it was found that at these very low flows surface tension and wave action of the headpool were of much more importance in the conveyance of small flow. It is the opinion of the author that the V-notch is completely impractical from any field standpoint.

Future Investigation

In the laboratory, all apparatus, test procedures, and analysis were completely satisfactory except for the simulated, corrugated metal section. It is the author's opinion that the method of coiling a wire

inside Lucite pipe to simulate corrugated metal conduit is not satisfactory. A slight variance of the spacing of the coils between the piezometer taps could easily result in a relatively large roughness variance. This procedure was successful to the extent that the general desired range of roughness was obtained. It is the author's opinion that if some means of fastening each coil to the Lucite pipe circumference was obtained, a more reliable and definite roughness could be produced. However, the adjustment of this roughness with a desired value would be a quite difficult procedure.

In the field, it will be necessary to continue data collection so that the rating curve can be completely substantiated. It will be necessary that the time-drive mechansim of the Parshall flume recorder be redesigned and a constant drive rate obtained. When a constant rate is obtained on this recorder, there will be no synchronization problem between the two recorders, and more reliable stage-discharge records can be obtained. The installation of the Parshall flume in the downstream channel is presently very sound, and it should withstand any record any future flow.

CONCLUSIONS

The following conclusions can be drawn from the investigation:

1. It can be concluded that the V-notch cast in the front lip of the spillway is completely impractical. Surface tension and wave action completely deteriorate the ability of the V-notch to convey small flows through the spillway.

2. It can be concluded that the increase in conduit roughness caused by the corrugated metal end section caused the spillway to prematurely flow full. It can further be concluded that the corrugated end section eliminated almost all slug flow through the spillway and caused an abrupt change of the spillway rating curve from weir flow to full-pipe flow.

3. It can be concluded that for the specific spillway, the weir flow portion of the spillway rating curve follows the form of the generally accepted weir flow equation, but it does not follow the variable coefficient broad-crested weir flow equation which was originally surmised. Instead, the weir flow portion of the rating curve has a constant coefficient, C, and the resulting equation is:

$$Q = 3.90\ h^{5/2}$$

Since the spillway flowed full prematurely, no slug flow was encountered. The full-pipe flow portion of the rating curve is very near the generally accepted form for full-pipe flow, and the resulting equation is:

$$Q = 4.75\ H^{0.57}$$

4. The theoretical and laboratory development of rating curves for the spillway are essentially equivalent as far as the rating curve form is concerned, but estimation of the loss coefficients for the predetermined theoretical rating curve resulted in a large variance between the originally surmised theoretical rating curve and the actual developed rating curve. Therefore, when it became possible to select loss coefficients from the model data, the theoretical and laboratory rating curves were essentially equivalent. The field data obtained was not sufficient for definite conclusions for comparison of the respective rating curves, although it can be concluded that the model-predicted rating curve is

definitely within the general range of the actual rating curve for the spillway. Figure XXI and XXII are graphically comparisons of the respective rating curves and data.

LITERATURE CITED

1. Albertson, Maurice L., et al., 1960, Fluid Mechanics for Engineers, Prentice-Hall, Inc., Englewood Cliffs, New Jersey, 567 p.

2. Allen, J., 1947, Scale Models in Hydraulic Engineering, Longmans, Green and Company, New York, p. 11-94.

3. Blaisdell, Fred W., 1958, Hydraulics of Closed Conduit Spillways, Part I, Theory and Its Application, Technical Paper No. 12, Series B., St. Anthony Falls Hydraulics Laboratory, University of Minnesota, 22 p.

4. Blaisdell, Fred W., 1950, Hydraulics of Drop Inlet Pipe Conduit Spillways, M. S. Thesis, University of New Hampshire.

5. Blaisdell, Fred W., and Donnelly, Charles A., 1951, Capacity of Box Inlet Drop Spillways, Technical Paper No. 7, Series B., St. Anthony Falls Hydraulics Laboratory, University of Minnesota, 36 p.

6. Blaisdell, Fred W., and Donnelly, Charles A., 1951, Hydraulic Design of the Box Inlet Drop Spillway, U. S. Department of Agriculture, Soil Conservation Service, Technical Paper No. 106, 53 p.

7. Buckingham, E., 1915, Experiments and Forms of Emperical Equations, Trans. A. S. M. E., Vol. 37.

8. Eckman, Donald P., 1961, Industrial Instrumentation, John Wiley & Sons, Inc., New York, p. 196-199.

9. Edwards, Donald P., 1961, Preliminary Results on the Hooded Ogee Pipe Drop Spillway, M. S. Thesis, South Dakota State College.

10. Frevert, Richard K., et al., 1959, Soil and Water Conservation Engineering, John Wiley & Sons, Inc., New York, p. 197-216.

11. Israelsen, Orson W., 1958, Irrigation Principles and Practices, John Wiley & Sons, Inc., New York, p. 48-49.

12. Kessler, Lewis H., 1934, Erosion Control of Structured Drop Inlets and Spillways, Research Bulletin 122, University of Wisconsin, 66 p.

13. King, Horace W., 1954, Handbook of Hydraulics, McGraw-Hill Book Company, Inc., New York.

14. Murphy, Glenn, 1950, Similitude in Engineering, The Ronald Press Company, New York, p. 17-174.

15. Nelson, Gerald H., 1956, Flow Regimes of a Drop Inlet Spillway, A. S. A. E. Journal 37:177-181.

16. Replogle, John A., 1961, Comparison of Theoretical, Laboratory, and Field Discharge Ratings of a Drop Inlet for a Small Farm Pond, Paper No. 61-703, Presented at 1961 Winter Meeting of A. S. A. E.

17. Rouse, Hunter, 1959, Advanced Mechanics of Fluids, McGraw-Hill Book Company, Inc., New York, p. 5-28.

18. Rouse, Hunter, 1938, Fluid Mechanics for Hydraulic Engineers, McGraw-Hill Book Company, Inc., New York, p. 86-130.

19. Rouse, Hunter, and Ince, Simon, 1957, History of Hydraulics, Iowa Institute of Hydraulic Research, State University of Iowa, p. 1-42.

20. United States Department of Agriculture, After a Hundred Years, The Yearbook of Agriculture, 1962, U. S. Government Printing Office, Washington, D. C., p. 151-208.

21. United States Department of Agriculture, Prepared by Soil Conservation Service, Preliminary Work Plan, Scott Creek Watershed, May, 1954.

22. Vennard, John K., 1958, Elementary Fluid Mechanics, John Wiley & Sons, Inc., New York, 401 p.

APPENDICES

APPENDIX A. DEFINITION OF SYMBOLS

Definition of Symbols:

A - full-pipe flow equation coefficient

a - area of conduit

C - broad-crested weir equation coefficient

D - diameter of pipe

e - roughness of pipe well

f_c - Darcy-Weisbach friction factor for corrugated metal pipe

f_f - Darcy-Weisbach friction factor for concrete pipe

f_l - Darcy-Weisbach friction factor for Lucite pipe

g - gravitation effect

H - total head lost through spillway

h - head above the lip of the spillway

h_L - head lost through the spillway

K_r - riser and transition loss coefficient

K_t - transition from smooth to rough conduit

L - length of respective spillway conduit

L_r - length ratio (L_m/L_p)

m - exponent of the head (H) of the full-pipe flow equation (slope of the logarithmic plot)

n - Manning friction coefficient

P - pressure

Q - spillway discharge

R - hydraulic radius

R_e - Reynolds number

S - conduit slope

S_f - specific gravity of manometer fluid

S_w - specific gravity of water

t - time recorded for given discharge

V - average flow velocity

V_r - average velocity ratio (V_m/V_p)

W - Parshall flume throat width

ρ - density of fluid

μ - dynamic viscosity of the fluid

ν - kinematic viscosity

γ - specific weight

APPENDIX B. MANOMETER DATA ANALYSIS

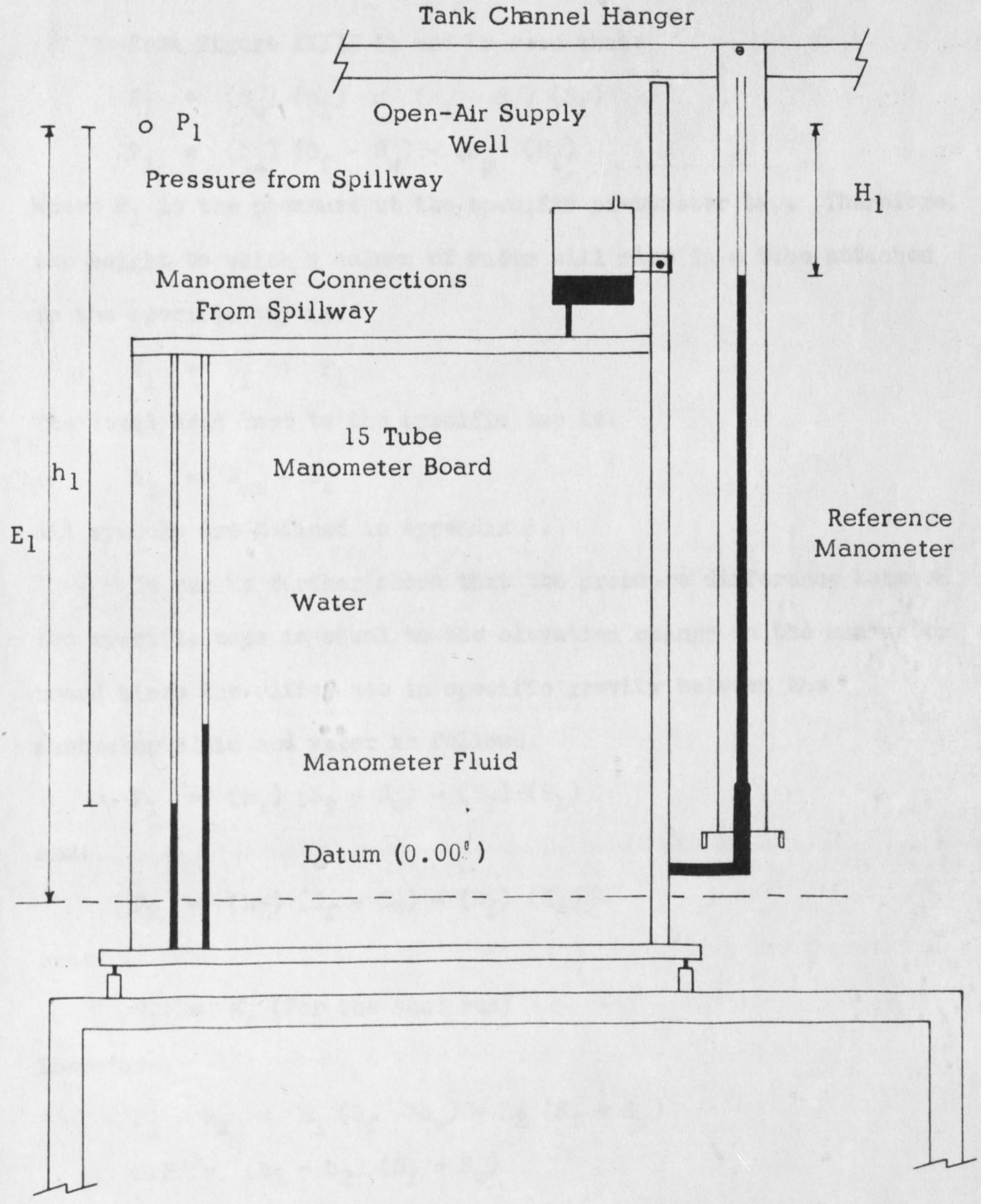

Figure XXIII. Schematic of Manometer Apparatus

From Figure XXIII it can be seen that:

$$P_1 + (S_w)(h_1) = (h_1 - H_1)(S_f)$$

$$P_1 = (h_1)(S_f - S_w) - (S_p)(H_1)$$

Where P_1 is the pressure at the specific piezometer tap. Therefore, the height to which a column of water will rise in a tube attached to the specific tap is:

$$Y_1 = E_1 + P_1$$

The total head lost to the specific tap is:

$$h_L = E_{ws} - E_1$$

All symbols are defined in Appendix A.

It can be further shown that the pressure difference between two specific taps is equal to the elevation change on the manometer board times the difference in specific gravity between the manometer fluid and water as follows:

$$P_1 = (h_1)(S_f - S_w) - (S_f)(H_1)$$

And:

$$P_2 = (h_2)(S_f - S_w) - (S_f)(H_2)$$

But:

$$H_1 = H_2 \text{ (For the same run)}$$

Therefore:

$$P_1 - P_2 = h_1(S_f - S_w) - h_2(S_f - S_w)$$

$$\Delta P = (h_1 - h_2)(S_f - S_w)$$

Sample calculations for data given in Table 2 for run number 108 are:

Piezometer tap 8:

$$P_8 = (60.192 - 17.392)(1.75) - 60.192 = 14.7"$$

$$Y_8 = 70.792 + 14.7 = 85.492"$$

$$h_L = 92.088 - 85.492 = 0.588'$$

And:

$$K_r = \frac{(h_L)(2g)}{V^2} = \frac{(0.558)(64.4)}{27.75} = 1.31$$

Piezometer tap 13:

$$P_{13} = (47.022 - 14.022)(1.75) - 47.022 = 10.728"$$

$$Y_{13} = 67.422 + 10.728 = 78.150"$$

$$h_L = 85.492 - 78.150 = 7.342" = 0.6118'$$

And:

$$f_1 = \frac{(D)(2g)}{(L)(V^2)} = \frac{(0.25)(64.4)}{(24)(27.75)} = 0.0148$$

Piezometer tap 14:

$$P_{14} = (41.003 - 13.753)(1.75) - 41.003 = 6.685"$$

$$Y_{14} = 67.153 + 6.685 = 73.838"$$

Since piezometer taps 13 and 14 were not located at the transition section from relative smooth conduit to rough, the average loss in these respective conduits were projected to the transition point and the head loss coefficient then calculated.

Therefore:

$$h_L = 78.150 - 73.838 = 4.312" - 1.360" = 2.952$$

$$= 0.246'$$

And:

$$K_t = \frac{(h_1)(2g)}{V^2_p} = \frac{(0.246)(64.4)}{27.75} = 0.571$$

Piezometer tap 15:

$$P_{15} = (37.922 - 13.472)(1.75) - 37.922 = 4.866"$$

$$Y_{15} = 66.872 + 4.866 = 71.738"$$

$$h_L = 73.838 - 71.738 = 2.100" = 0.175'$$

And:

$$f_c = \frac{(D)(2g)}{(L)(V^2)} = \frac{(0.25)(64.4)}{(3.33)(27.75)} = 0.0508$$

The Reynolds number (R_e) is calculated:

$$R_e = \frac{VD}{\nu} = \frac{(5.27)(0.25)}{1.03 \times 10^5} = 1.279 \times 10^5$$

APPENDIX C. INSTRUMENTATION CIRCUIT DIAGRAMS

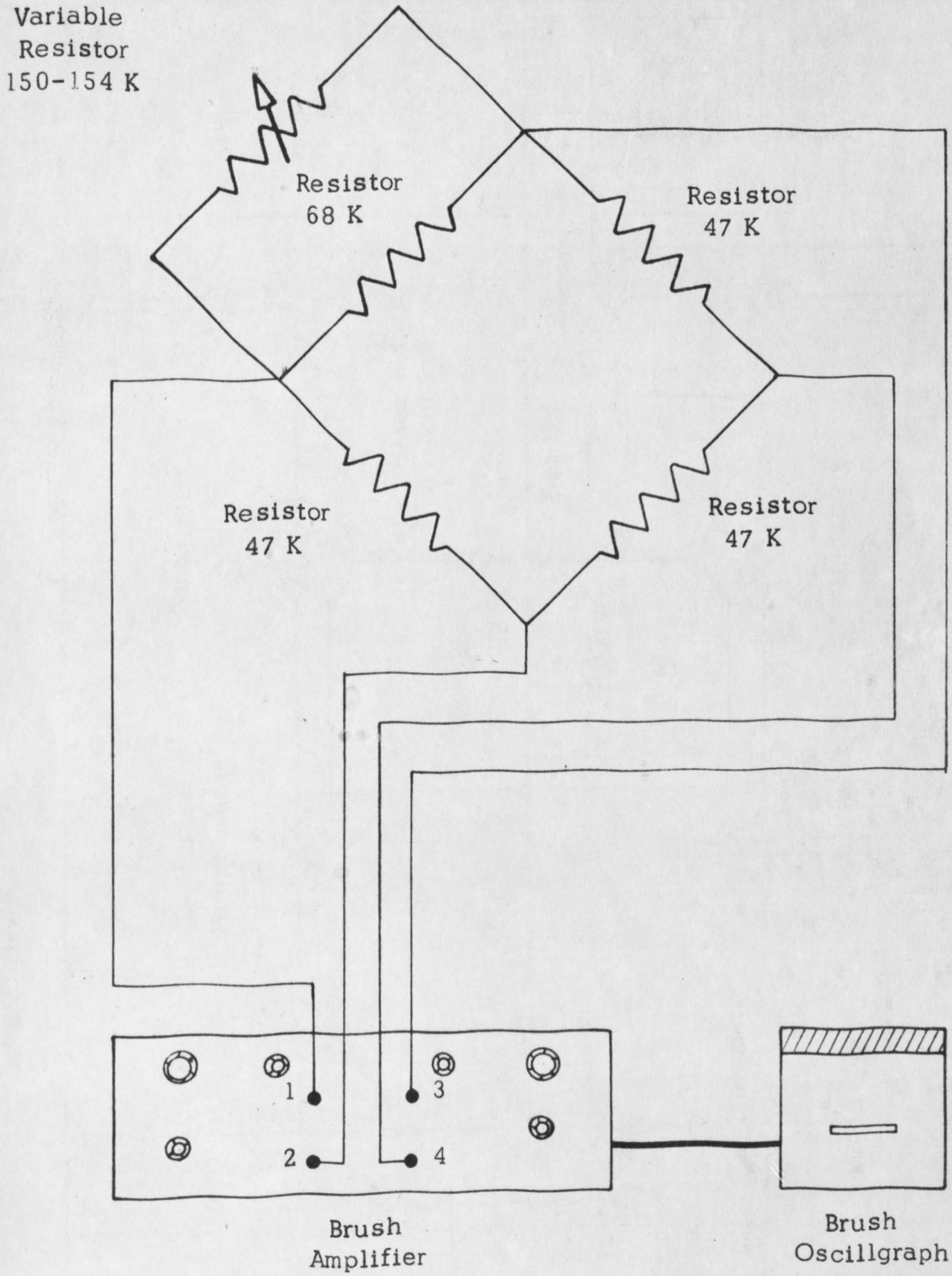

Figure XXIV. Schematic Circuit Diagram for the Discharge Recorder

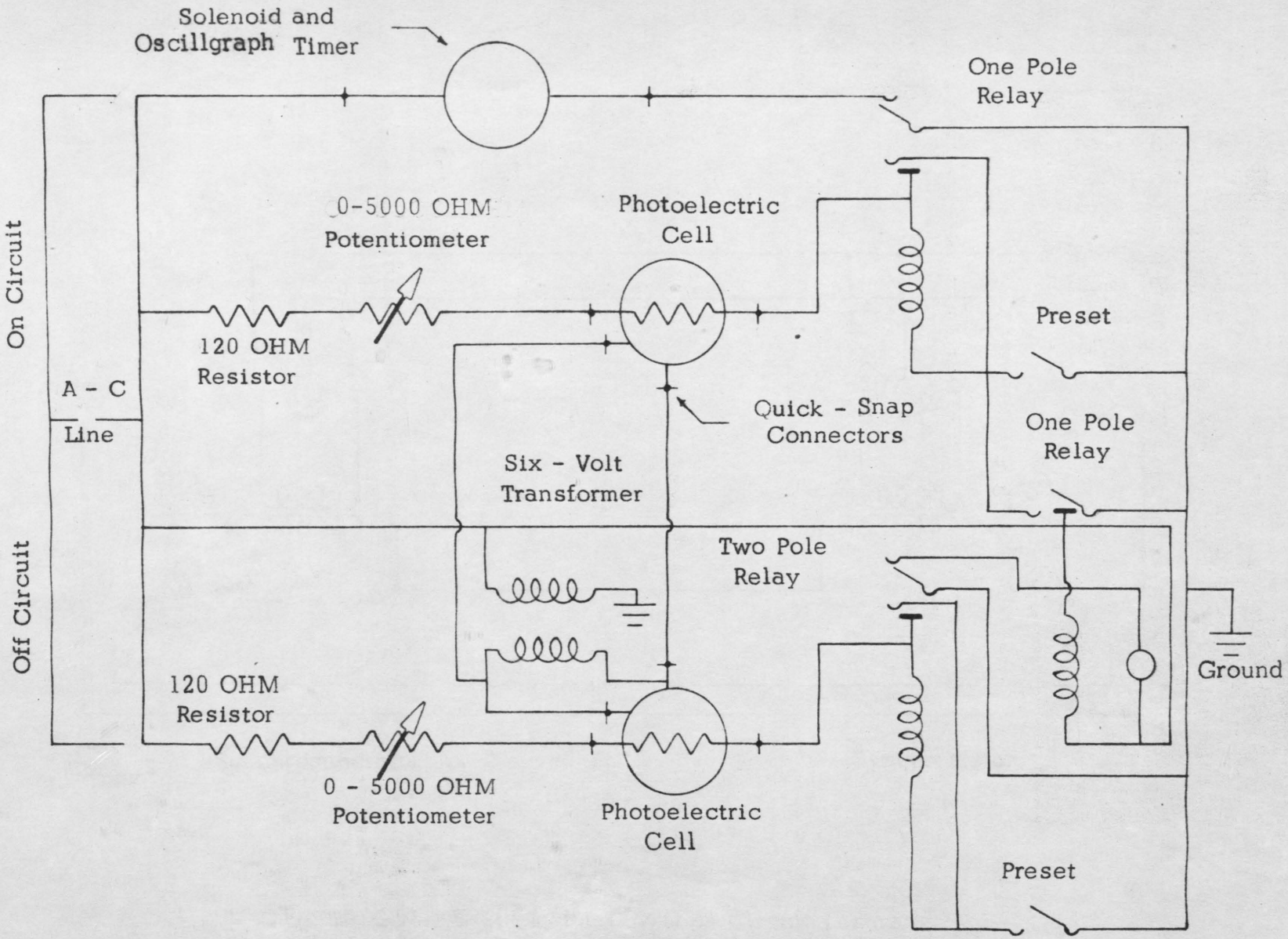

Figure XXV. Circuit Diagram for the Photoelectric Cell Unit

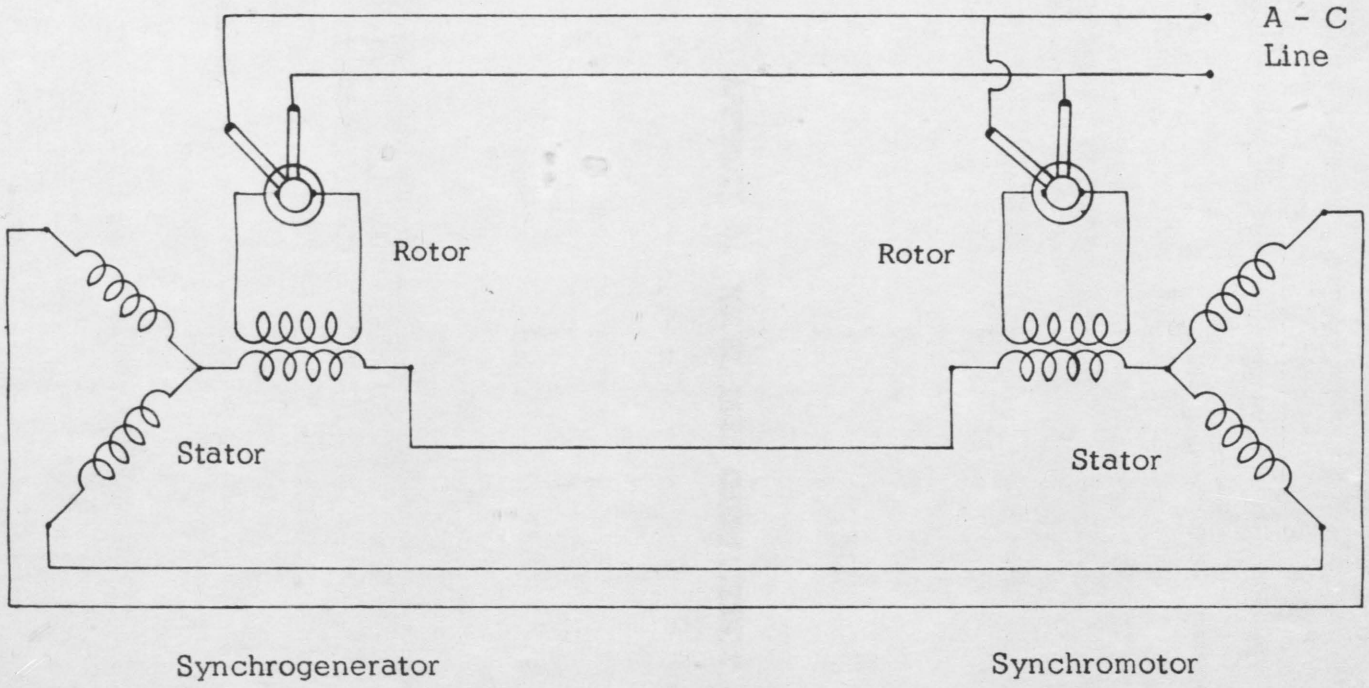

Figure XXVI. Basic Synchro System Circuit Diagram

APPENDIX D. MODEL LOSS COEFFICIENTS

Table 6. Model Loss Coefficients

Run No.	Q_m (cfs)	h_m (ft.)	K_r	f_l	K_t	f_c
46	0.2495	0.2670	1.28	0.0149	0.676	0.0507
47	0.2478	0.2777	1.31	0.0152	0.578	0.0527
48	0.2495	0.2890	1.30	0.0154	0.591	0.0507
49	0.2528	0.2980	1.28	0.0147	0.567	0.0507
50	0.2891	0.2980	1.29	0.0112	0.433	0.0387
51	0.2528	0.3040	1.27	0.0149	0.578	0.0495
52	0.2528	0.3080	1.32	0.0145	0.578	0.0406
53	0.2891	0.3110	0.97	0.0114	0.451	0.0378
55	0.2934	0.3180	0.98	0.0108	0.438	0.0376
56	0.2528	0.3190	1.28	0.0149	0.589	0.0495
57	0.2528	0.3200	1.27	0.0149	0.589	0.0507
58	0.2533	0.3520	1.92	0.0109	0.590	0.0529
59	0.2562	0.3530	1.87	0.0104	0.598	0.0517
60	0.2562	0.3590	1.88	0.0104	0.532	0.0641
61	0.2562	0.3600	1.89	0.0105	0.598	0.0517
62	0.2461	0.3600	1.86	0.0111	0.608	0.0561
63	0.2523	0.3610	1.77	0.0107	0.578	0.0533
65	0.2562	0.3610	1.71	0.0104	0.442	0.0665
66	0.2533	0.3620	1.75	0.0106	0.638	0.0517
67	0.2533	0.3635	1.75	0.0107	0.612	0.0529
68	0.2533	0.3540	1.75	0.0107	0.588	0.0568
69	0.2562	0.3520	1.69	0.0102	0.598	0.0517
70	0.2533	0.3555	1.73	0.0104	0.600	0.0568
84	0.2420	0.1920	1.04	0.0156	0.390	0.0530
85	0.2402	0.1670	1.06	0.0152	0.566	0.0569
86	0.2385	0.1560	1.10	0.0148	0.545	0.0532
87	0.2328	0.1560	1.19	0.0152	0.565	0.0570
88	0.2385	0.1710	1.15	0.0142	0.556	0.0531
89	0.2416	0.1930	1.06	0.0145	0.532	0.0542
90	0.2429	0.2190	1.06	0.0143	0.549	0.0536
91	0.2429	0.2280	1.07	0.0145	0.590	0.0522
92	0.2528	0.2370	0.98	0.0136	0.503	0.0504
93	0.2461	0.2460	1.06	0.0144	0.541	0.0532
94	0.2457	0.2350	1.09	0.0144	0.510	0.0544
95	0.2430	0.2230	1.10	0.0146	0.531	0.0536
96	0.2416	0.2110	1.15	0.0143	0.553	0.0552
97	0.2402	0.2040	1.13	0.0148	0.560	0.0559

Table 6. (continued)

Run No.	Q_m (cfs)	h_m (ft.)	K_r	f_l	K_t	f_c
98	0.2385	0.1950	1.13	0.0153	0.553	0.0566
99	0.2385	0.1880	1.17	0.0147	0.548	0.0566
100	0.2385	0.1780	1.17	0.0146	0.543	0.0566
101	0.2385	0.1730	1.15	0.0147	0.534	0.0556
102	0.2371	0.1700	1.13	0.0153	0.533	0.0562
105	0.2650	0.4650	1.53	0.0145	0.561	0.0491
106	0.2596	0.4500	1.33	0.0147	0.603	0.0469
108	0.2581	0.4200	1.31	0.0148	0.571	0.0508
109	0.2581	0.4080	1.27	0.0151	0.587	0.0492
110	0.2561	0.3980	1.34	0.0147	0.581	0.0490
111	0.2561	0.3870	1.25	0.0154	0.500	0.0682
112	0.2547	0.3780	1.30	0.0153	0.581	0.0505
113	0.2547	0.3700	1.37	0.0142	0.590	0.0505
114	0.2547	0.3720	1.34	0.0144	0.588	0.0514
115	0.2554	0.3810	1.48	0.0129	0.591	0.0503
116	0.2585	0.3850	1.32	0.0140	0.582	0.0492
117	0.2560	0.3900	1.35	0.0150	0.653	0.0323
118	0.2560	0.3960	1.31	0.0149	0.600	0.0418
119	0.2568	0.3990	1.28	0.0151	0.650	0.0321
120	0.2578	0.4020	1.27	0.0133	0.731	0.0511
121	0.2578	0.4040	1.25	0.0134	0.799	0.0365
123	0.2652	0.4920	1.25	0.0146	0.574	0.0483
124	0.2633	0.4950	1.29	0.0144	0.594	0.0507
125	0.2614	0.4960	1.25	0.0155	0.583	0.0523
126	0.2633	0.5000	1.29	0.0145	0.574	0.0507
127	0.2689	0.5010	1.21	0.0144	0.555	0.0493
128	0.2659	0.5040	1.21	0.0147	0.574	0.0504
129	0.2678	0.5040	1.23	0.0143	0.581	0.0482
132	0.2652	0.5060	1.28	0.0143	0.583	0.0500
133	0.2659	0.5390	1.22	0.0150	0.587	0.0504
135	0.2728	0.5630	1.21	0.0139	0.573	0.0479
136	0.2688	0.5720	1.24	0.0147	0.594	0.0487
137	0.2728	0.5800	1.20	0.0144	0.573	0.0490
138	0.2688	0.5860	1.25	0.0146	0.590	0.0506
139	0.2714	0.5910	1.24	0.0143	0.600	0.0484
140	0.2707	0.5990	1.22	0.0148	0.590	0.0498
141	0.2688	0.6010	1.28	0.0146	0.605	0.0514

Table 6. (continued)

Run No.	Q_m (cfs)	h_m (ft.)	K_r	f_l	K_t	f_c
142	0.2728	0.6060	1.21	0.0144	0.592	0.0490
143	0.2728	0.6080	1.23	0.0143	0.602	0.0479
144	0.2728	0.6090	1.23	0.0144	0.598	0.0471
145	0.2728	0.6140	1.24	0.0144	0.596	0.0479
146	0.2738	0.6160	1.23	0.0141	0.598	0.0476
147	0.2747	0.6220	1.22	0.0145	0.624	0.0474
148	0.2776	0.6230	1.21	0.0139	0.587	0.0474
149	0.2714	0.6050	1.29	0.0146	0.617	0.0476
150	0.2727	0.6210	1.29	0.0143	0.610	0.0471
151	0.2709	0.6180	1.27	0.0148	0.630	0.0478
153	0.2860	0.8400	1.33	0.0141	0.667	0.0447
154	0.2848	0.8460	1.34	0.0141	0.649	0.0450
155	0.2848	0.8550	1.35	0.0142	0.660	0.0464
156	0.2870	0.8640	1.35	0.0142	0.649	0.0456
157	0.2860	0.8700	1.30	0.0141	0.662	0.0461
158	0.2848	0.8740	1.36	0.0141	0.658	0.0464
159	0.2848	0.8740	1.35	0.0144	0.683	0.0450
160	0.2819	0.8140	1.33	0.0141	0.668	0.0459
162	0.2786	0.7810	1.29	0.0154	0.660	0.0468
163	0.2781	0.7690	1.29	0.0154	0.659	0.0487
164	0.2781	0.7580	1.37	0.0147	0.673	0.0480
165	0.2748	0.7480	1.33	0.0149	0.665	0.0498
167	0.2767	0.7350	1.30	0.0147	0.648	0.0491
168	0.2767	0.7110	1.31	0.0144	0.637	0.0491
169	0.2747	0.6820	1.34	0.0139	0.636	0.0483
172	0.2709	0.6820	1.31	0.0153	0.651	0.0497
173	0.2714	0.6800	1.33	0.0150	0.657	0.0476
174	0.2728	0.6770	1.35	0.0143	0.648	0.0479
176	0.2740	0.7110	1.35	0.0143	0.647	0.0499
178	0.2767	0.7300	1.35	0.0143	0.617	0.0491
179	0.2795	0.7410	1.35	0.0138	0.652	0.0467
180	0.2776	0.7450	1.34	0.0142	0.661	0.0474
182	0.2767	0.7760	1.33	0.0148	0.656	0.0491
183	0.2787	0.7880	1.35	0.0144	0.677	0.0478
184	0.2787	0.7970	1.36	0.0145	0.677	0.0478
185	0.2776	0.8060	1.34	0.0151	0.676	0.0489
186	0.2826	0.8183	1.39	0.0144	0.679	0.0446

Table 6. (continued)

Run No.	Q_m (cfs)	h_m (ft.)	K_r	f_l	K_t	f_c
187	0.2826	0.8240	1.33	0.0142	0.664	0.0471
188	0.2864	0.8510	1.32	0.0148	0.668	0.0494
189	0.2826	0.8520	1.31	0.0145	0.658	0.0478
190	0.2838	0.8390	1.33	0.0144	0.623	0.0467
191	0.2826	0.8410	1.29	0.0148	0.683	0.0463
192	0.2838	0.8480	1.34	0.0143	0.644	0.0453
193	0.2838	0.8560	1.34	0.0144	0.671	0.0467
194	0.2862	0.8600	1.31	0.0142	0.680	0.0445
195	0.2851	0.8620	1.32	0.0142	0.669	0.0463
196	0.2851	0.8660	1.31	0.0145	0.679	0.0455
197	0.2872	0.8770	1.31	0.0142	0.671	0.0456
198	0.2872	0.8870	1.29	0.0145	0.669	0.0422
199	0.2862	0.9030	1.37	0.0141	0.671	0.0459
200	0.2891	0.9150	1.29	0.0144	0.666	0.0450
201	0.2839	0.8430	1.31	0.0142	0.670	0.0467
202	0.2860	0.8440	1.31	0.0140	0.652	0.0497
205	0.2839	0.8500	1.30	0.0147	0.688	0.0460
207	0.2860	0.8710	1.32	0.0143	0.662	0.0475
208	0.2880	0.8730	1.34	0.0136	0.681	0.0469
209	0.2880	0.8840	1.30	0.0140	0.669	0.0469
210	0.2880	0.8970	1.33	0.0142	0.663	0.0469
211	0.2890	0.9090	1.31	0.0143	0.673	0.0476
212	0.2900	0.9210	1.29	0.0142	0.685	0.0447
214	0.2940	0.9460	1.33	0.0133	0.671	0.0455
215	0.2940	0.9520	1.26	0.0146	0.680	0.0423
216	0.2950	0.9580	1.30	0.0137	0.651	0.0459
218	0.2975	0.9740	1.31	0.0136	0.674	0.0443
220	0.2940	1.0140	1.35	0.0140	0.694	0.0449
221	0.2940	1.0270	1.30	0.0145	0.685	0.0449
222	0.3009	1.0430	1.27	0.0136	0.666	0.0429
244	0.2985	1.0920	1.31	0.0141	-----	------
245	0.3008	1.1340	1.32	0.0139	-----	------
246	0.3030	1.1640	1.33	0.0138	-----	------
247	0.3030	1.1860	1.28	0.0146	-----	------
249	0.3040	1.2230	1.27	0.0150	-----	------
250	0.3252	1.2360	1.16	0.0125	-----	------
253	0.3100	1.2830	1.29	0.0141	-----	------

Table 6. (continued)

Run No.	Q_m (cfs)	h_m (ft.)	K_T	f_1	K_t	f_c
254	0.3100	1.2900	1.27	0.0143	-----	------
255	0.3123	1.2970	1.28	0.0139	-----	------
257	0.3123	1.3150	1.28	0.0140	-----	------
258	0.3112	1.3160	1.30	0.0139	-----	------
259	0.3123	1.3240	1.27	0.0145	-----	------
260	0.3123	1.3260	1.26	0.0145	-----	------
261	0.3079	1.3040	1.32	0.0143	-----	------
262	0.3079	1.2790	1.31	0.0144	-----	------
263	0.3079	1.2550	1.35	0.0136	-----	------
264	0.3063	1.2270	1.32	0.0139	-----	------
265	0.3040	1.2090	1.31	0.0142	-----	------
266	0.3030	1.1910	1.28	0.0145	-----	------
267	0.3020	1.1770	1.28	0.0144	-----	------
268	0.3010	1.1300	1.29	0.0139	-----	------
269	0.2985	1.0630	1.22	0.0146	-----	------
270	0.2975	1.0040	1.28	0.0135	-----	------
271	0.2930	0.9510	1.29	0.0136	-----	------
272	0.2880	0.8980	1.30	0.0140	-----	------
273	0.2858	0.8540	1.31	0.0139	-----	------
274	0.2830	0.8140	1.31	0.0141	-----	------
275	0.2820	0.7810	1.28	0.0143	-----	------
276	0.2678	0.5770	1.31	0.0144	0.637	0.0510
277	0.2685	0.5700	1.27	0.0147	0.628	0.0495
278	0.2670	0.5660	1.29	0.0147	0.637	0.0511